Engineering Structures 265 (2022) 114427

Contents lists available at ScienceDirect

Engineering Structures

journal homepage: www.elsevier.com/locate/engstruct

Quantifying robustness in tall timber buildings: A case study

Konstantinos Voulpiotis *, Styfen Schär, Andrea Frangi

Institute of Structural Engineering (IBK), Swiss Federal Institute of Technology (ETH), HIL E43.2, Stefano-Franscini-Platz 5, CH-8093 Zurich, Switzerland

ARTICLE INFO

Keywords:
Disproportionate collapse
Tall timber
System effects
Risk
Reliability
Classification
Sensitivity study

ABSTRACT

Robustness research has become popular, however very little is known on its explicit quantification. This paper summarises a quantification method previously published by the main author and proceeds in demonstrating its step-by-step application with a case study tall timber building. A hypothetical 15-storey post-and-beam timber building with a central core is designed for normal loads, and four improved options are designed to account for abnormal loads in order to increase the building's robustness. A detailed, nonlinear, dynamic Finite Element model is set up in Abaqus® to model three ground floor column removal scenarios, and a Random Forest classifier is set up to propagate uncertainties, to efficiently estimate the probability of certain collapse classes occurring, and to calculate the importance of each input parameter. The results show how design improvements at the whole building scale (e.g., strong floors) have a higher impact on robustness performance than just improving the strength and ductility of some selected connections, although these results are exclusive to the building studied. The case study reinforces the importance of a sound conceptual design for achieving robustness in tall timber buildings.

1. Introduction

Our profession is seeing a paradigm shift towards buildings of lower carbon footprint: tall timber buildings are a fine example of this shift. Any departure from the "familiar waters" of the common structural typologies runs a higher risk of not having identified or anticipated certain structural behaviours: similar to the scaling issues that led to the partial collapse of the Ronan Point in London in 1968 [1], we must understand how timber buildings scale to the new heights constructed in the last 10 years, particularly regarding their disproportionate collapse behaviour.

Structural robustness, or disproportionate collapse resistance, is the ability of a structure to withstand damage without disproportionate further consequences, and it is an important and yet not so widely understood quality of our building stock. While a lot of work has been put in understanding structural robustness at a qualitative level and regarding concrete and steel buildings, little is known on the robustness of timber buildings and even less on how to specifically quantify how robust is a building, and whether this is enough or not. Initial studies focused on medium-rise CLT buildings have identified connection ductility as a key requirement to enable catenary action in beams and floors, an efficient way to redistribute loads in case of damage.

The goal of this paper is to build on the fledging research of the topic by numerically analysing an example case study of a post-and-beam tall timber building with a central core. The analysis will aim to quantify robustness following an adaptation of the method presented in Voulpiotis et al. (2021) [2]. Section 2 summarises the current state of the art and describes the quantification procedure. Section 3 details and justifies the use of each modelling technique to achieve our quantification goal. The results are presented and discussed together with the model limitations in Section 4, followed by conclusions in Section 5. For more details on the case study and a connection with robustness design recommendations for tall timber buildings, please refer to the doctoral thesis of Voulpiotis (2021) [3].

2. State of the art and methodology

2.1. Structural design and analysis for robustness

Resistance to disproportionate collapse is best understood by looking at the mechanics of load redistributions when a structure is subjected to damage. A building which is able to redistribute the loads away from a damaged member and safely back down to the ground without collapsing is said to be robust to this damage scenario. The most desirable structural quality that can help in this is the catenary action of beams and membrane action of slabs as they deform significantly. It is therefore imperative that members and connections have to withstand

* Corresponding author.
E-mail addresses: voulpiotis@ibk.baug.ethz.ch (K. Voulpiotis), styfen.schaer@ibk.baug.ethz.ch (S. Schär), frangi@ibk.baug.ethz.ch (A. Frangi).

https://doi.org/10.1016/j.engstruct.2022.114427
Received 3 February 2022; Received in revised form 8 April 2022; Accepted 17 May 2022
Available online 14 June 2022

high deformations while maintaining load carrying capacity. An overview of the beam/floor load redistribution mechanisms is shown in Fig. 1 below, adapted from the doctoral thesis of Mpidi Bita (2019) [4].

Ensuring the existence and functionality of these alternative load paths can be achieved using direct or indirect design methods, summarised below (see Fig. 2).

It is possible to use the methods above only qualitatively to come up with a robust conceptual design, as detailed in Voulpiotis et al. (2021) [2]. Numerical modelling is, of course, an additional analysis step that can prove the existence of the alternative load paths and demonstrate the fitness of various structural solutions. It is typically carried out in a deterministic manner, where a building is modelled in various column removal damage scenarios.

A nonlinear dynamic numerical model is best suited to study the flow of loads in a structure including post-critical behaviour. However, it is normally computationally expensive and complicated, which has led engineers to reach various compromises by simplifying to linear and/or static models with the necessary dynamic amplification factors, or hybrid combinations thereof, such as static-pushover analyses where the dynamic effects are estimated using an energy balance approach. Byfield *et al.* (2014) [5] offer an extensive review of these analysis methods. How these methods are used in the overall robustness research, including verification by experiments, is extensively discussed in the review paper of Adam et al. (2018) [6].

2.2. Robustness of tall timber buildings and the importance of connections

Current design guidance on robustness (EN 1991-1-7:2006 [7], ASCE 7-22 [8], UFC 2016 [9], for an overview see Mpidi Bita et al. (2019) [10]) is heavily influenced by concrete and steel building research following the partial collapse of the Ronan Point Tower in London in 1968 [11]. The increasing popularity of Engineered Wood Products (EWPs), largely due to their prefabrication and sustainability possibilities, has led to the construction of new tall timber building typologies [12], where the development of alternative load paths is largely unstudied [13]. When applied to timber buildings, the existing guidance has been proven to be uneconomic and often unconservative [14].

Despite the scarcity of guidelines for timber buildings, several modern tall timber projects have explicitly implemented design methodologies to increase robustness. Some examples are: the provision of vertical tie forces by designing the column-column connections to carry tension loads (Brock Commons residence, Canada [15]); the provision of alternative load paths with the design of two-way spanning floor slabs acting as cantilevers and walls in both directions acting as deep beams in case of column loss (Stadthaus, London [16]) as studied by Milner et al. (1998) [17]; and the compartmentalisation of the building such that damage propagation is arrested in predefined boundaries (Treet, Norway [18]). More examples are provided by Mpidi Bita et al. (2022) [19], who also provide a review of the current research on the disproportionate collapse resistance of tall timber buildings. These largely consist of whole-building numerical models in collapse scenarios, a complex undertaking which was first attempted in tall timber buildings by Mpidi Bita (2019) [4]. Detailed studies on two CLT buildings of nine and twelve storeys respectively [20,21] demonstrated that disproportionate collapse prevention requires higher tie forces than what the structures could offer with conventional design that does not explicitly take into account element loss. This led to specific tie force recommendations for multi-storey CLT buildings with emphasis on the importance of connection detailing to enable catenary action of floors and beams [22]. The importance of the connection ductility led to the development of a novel floor-floor connection [23] whose ductile performance was demonstrated in physical experiments [24]. Huber et al. (2021) [25] modelled this novel connection in a parametric environment and examined the effect of different boundary conditions on the load redistribution mechanisms of a typical multi-storey CLT building designed to European standards. With a more detailed look into the micro-modelling of connections in European CLT construction, Huber et al. [26] studied the alternative load paths in multi-storey CLT buildings, finding that the most common are transverse shear action of the floors, arching (deep beam) action of the walls, and catenary action of the floors. A more recent study [27] has focused on the implementation of linear static Alternative Load Path Analysis according to the GSA 2013 [28] and UFC 2016 [9] standards. Determining an accurate Dynamic Amplification Factor (DAF; that is, the ratio between the maximum dynamic response to the quasi-static response of the structure) is important for being able to simplify nonlinear dynamic problems to linear static ones. A parametric study by Cao et al. (2021) [29] found the DAF to be approximately 2.0 for timber frames, mainly influenced by the structures' damping ratio and connection stiffness. Damping in tall timber buildings is still not fully understood, which has attracted a lot of new research [30].

The prevention of disproportionate collapse in tall timber buildings

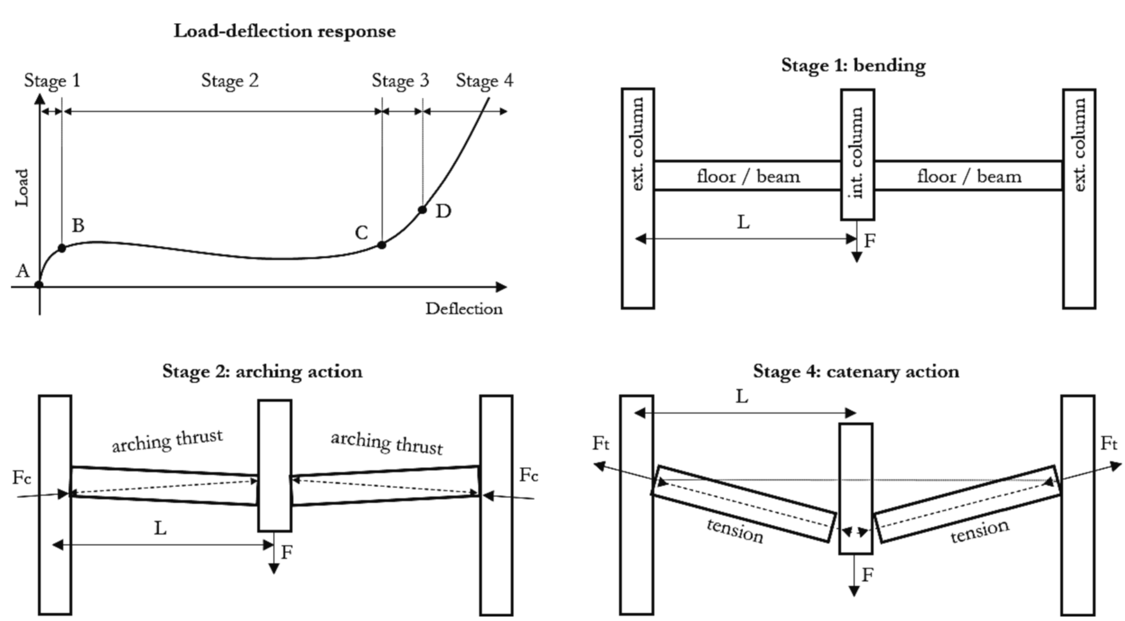

Fig. 1. Load redistribution of a constrained beam or floor (adapted from Mpidi Bita, 2019 [4]).

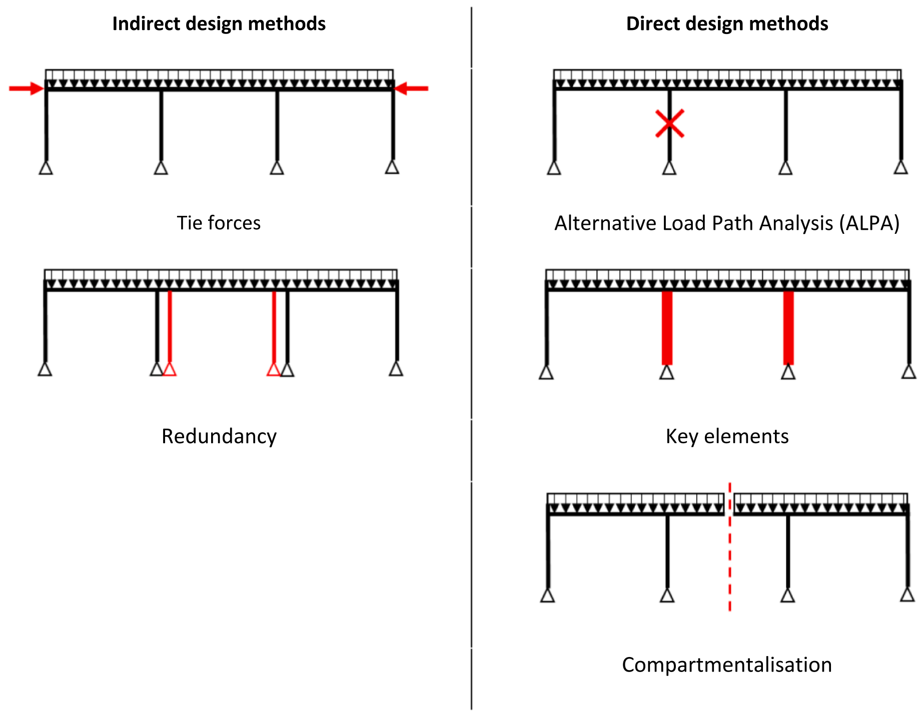

Fig. 2. Direct and indirect robustness design methods.

in fire scenarios (slow element removal and systematic rather than localised damage) has also recently gained attention with qualitative studies [31] following the framework of Voulpiotis (2021) [2], as well as detailed numerical studies [32,33].

While experiments are rare, the research group of Lyu, Cheng, et al. have tested several ¼ scale 2D and 3D timber frames in corner, edge, and middle column removal scenarios [34–37]. The experiments reinforced the importance of connection ductility to develop catenary action in beams and floors, and of floor slabs to redistribute loads and improve collapse resistance.

The common factor in the aforementioned research is the crucial role of connections in redistributing loads. Already before the research on tall timber buildings gained momentum, Dietsch (2011) [38] made recommendations on increasing the robustness of long-span timber structures, many of which regard the detailing of connections. The important role of moment-carrying timber connections in redistributing loads in statically indeterminate structures has been highlighted by Leijten (2011) [39]. The performance requirements of connections in earthquake scenarios has pushed timber research in earthquake-prone areas, such as New Zealand and Italy, towards finding structural solutions that are ductile, i.e. are able to deform significantly while maintaining load carrying capacity [40]. Given the brittleness of timber in bending and tension, ductility can be best achieved in timber connections where ductile steel parts are designed to fail before brittle timber does (overstrength design) [41]. Malo et al. (2011) [42] have discussed ductility in the context of disproportionate collapse, and made recommendations on how to measure it. Ottenhaus et al. (2021) [43] also provide a review of the ductility requirements for timber connections and proposed an “idealised load–displacement curve”.

2.3. Robustness quantification

Disproportionate collapse belongs to the category of extreme (rare) events, it is thus best studied in a probabilistic manner. Several frameworks to quantify robustness have been proposed in the last 30 years [2,44–47], all based on the calculation of a so-called robustness index which is used to compare the risk of secondary consequences to the risk of an initial damage. Fig. 3 demonstrates the sequence of events that can lead to a disproportionate collapse and how each step is quantified using conditional probabilities [48].

The robustness index defined by Baker et al. (2007) [46] is given by equation (1):

$$I_{Rob} = \frac{C_{Dir}}{C_{Dir} + P(C|D) \times C_{Ind}} \tag{1}$$

According to Voulpiotis et al. (2021) [2] we can measure the consequences in terms of extent of collapse area ($C_{Dir/Ind} \rightarrow A_{Fail,Dir/Ind}$). Since a damaged building can fail in different ways (“collapse classes”, Fig. 4), we calculate the robustness index for a given damage scenario by summing the indirect risk occurring from every collapse class i:

$$I_{Rob} = \frac{A_{Fail,Dir}}{A_{Fail,Dir} + \sum_{i=0}^{n} (P(C_i|D) \times A_{Fail,Ind,i})} \tag{2}$$

The calculation of an average robustness index across multiple damage scenarios follows an iterative procedure as depicted in Fig. 5.

The average robustness index, $I_{Rob(av)}$, is the sum of the robustness indices for individual damage scenarios, $I_{Rob(i)}$, weighted against the relative probability of each damage scenario i occurring, $W_{scen,i}$:

$$I_{Rob(av)} = \sum_{i=1}^{n} (W_{scen,i} \times I_{Rob(i)}) \tag{3}$$

where

$$W_{scen,i} = \frac{P_{scen,i}}{\sum_{i=1}^{n} P_{scen,i}} = \frac{(P(E) \times P(D|E))_i}{\sum_{i=1}^{n} (P(E) \times P(D|E))_i} \tag{4}$$

$P_{scen,i}$ is the probability of the i th scenario occurring, however we do not need to know the exact probability of the event exposure and initial damage: the relative probability between scenarios suffices.

By directly comparing the average robustness indices between different building designs we can draw conclusions about the increase (or decrease) in robustness of a building in different design decisions (Voulpiotis et al. 2021 [2]).

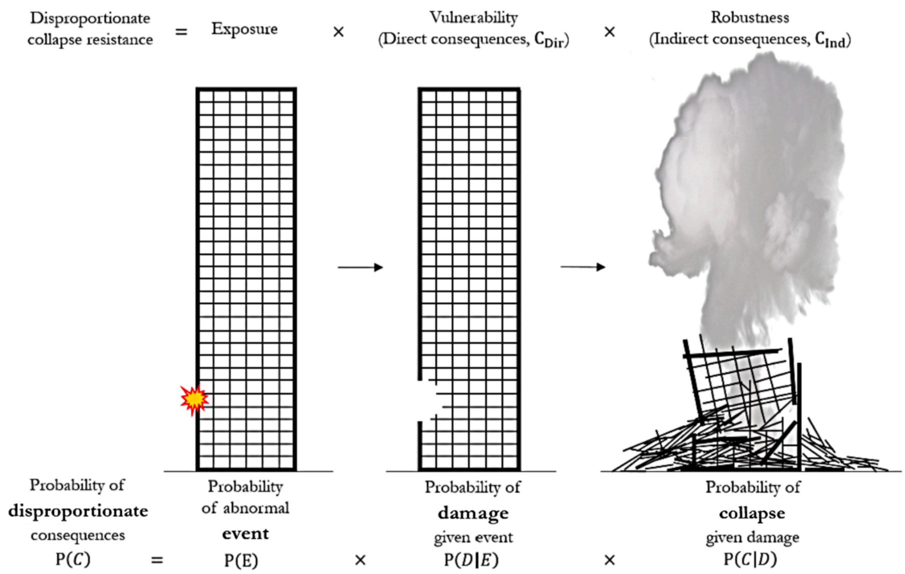

Fig. 3. Chain reaction of abnormal events potentially leading to collapse (adapted from EN 1991-1-7:2006 [7]).

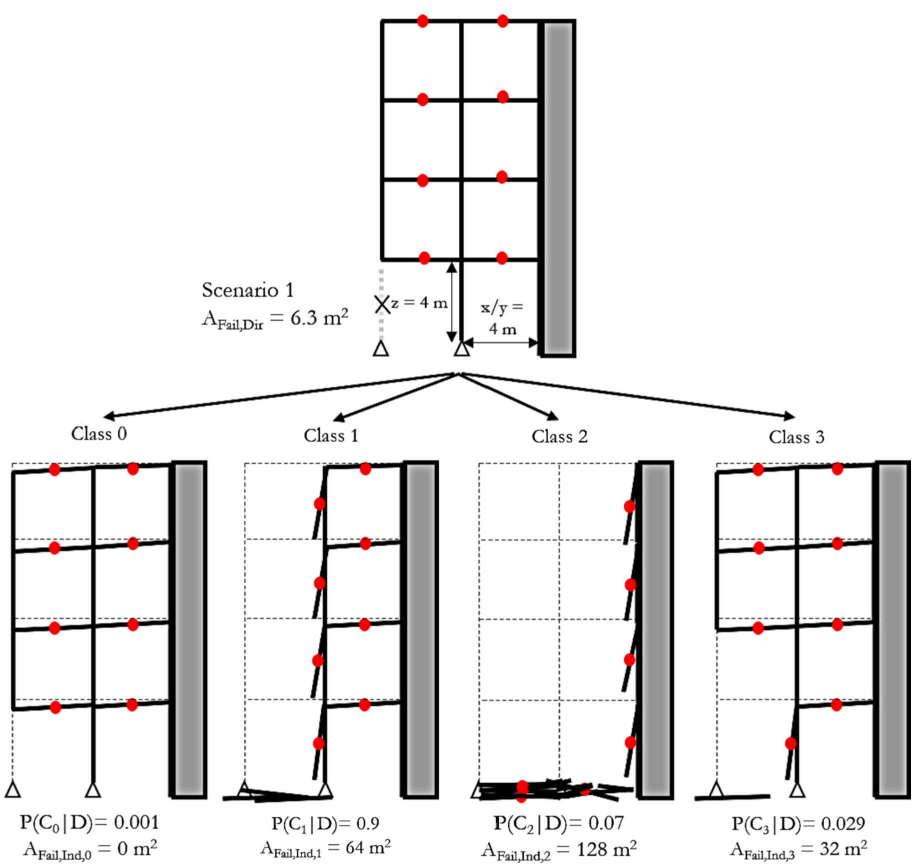

Fig. 4. Classification of possible collapses of an imaginary four-storey frame given an edge column removal. Here the probabilities are indicative only.

3. Case study example model setup

In Section 2 we saw that an accurate robustness quantification requires: (i) accurate input variables; (ii) a numerical model able to account for highly nonlinear, dynamic behaviour; and (iii) an uncertainty propagation method able to predict the probability of occurrence of different collapse classes. We have employed advanced numerical techniques to address each of these requirements efficiently. We have: (i) designed a tall timber building in great detail regarding its connections, to justify the critical model inputs; (ii) set up a detailed, nonlinear, dynamic Finite Element model such that we can analyse damage scenarios and follow the development of alternative load paths during the initial stages of collapse; and (iii) set up a classification meta-model, such that we can predict the occurrence of collapse classes without excessive CPU usage. These three steps are detailed in the three subsections below.

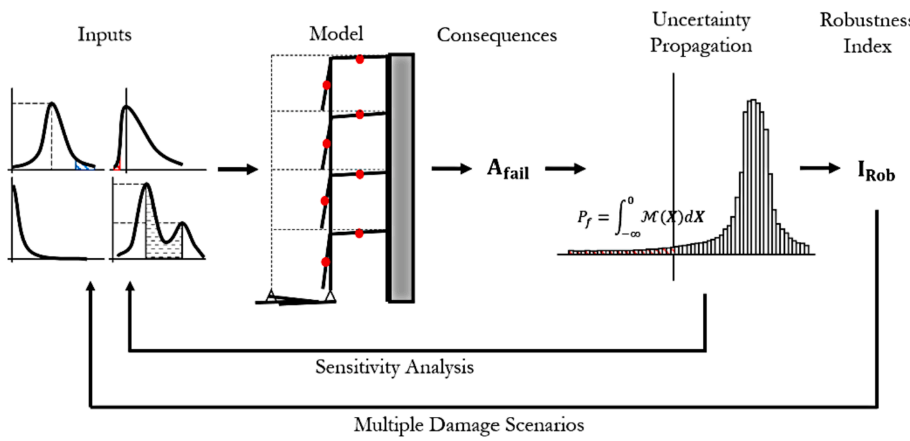

Fig. 5. Robustness index calculation workflow for every damage scenario.

3.1. Design of case study building

A hypothetical 15-storey timber building skeleton structure in Zürich, Switzerland, is designed to the Swiss standards to quantify its robustness using the method described in the previous chapter. The design is kept as simple as possible to focus on the collapse performance.

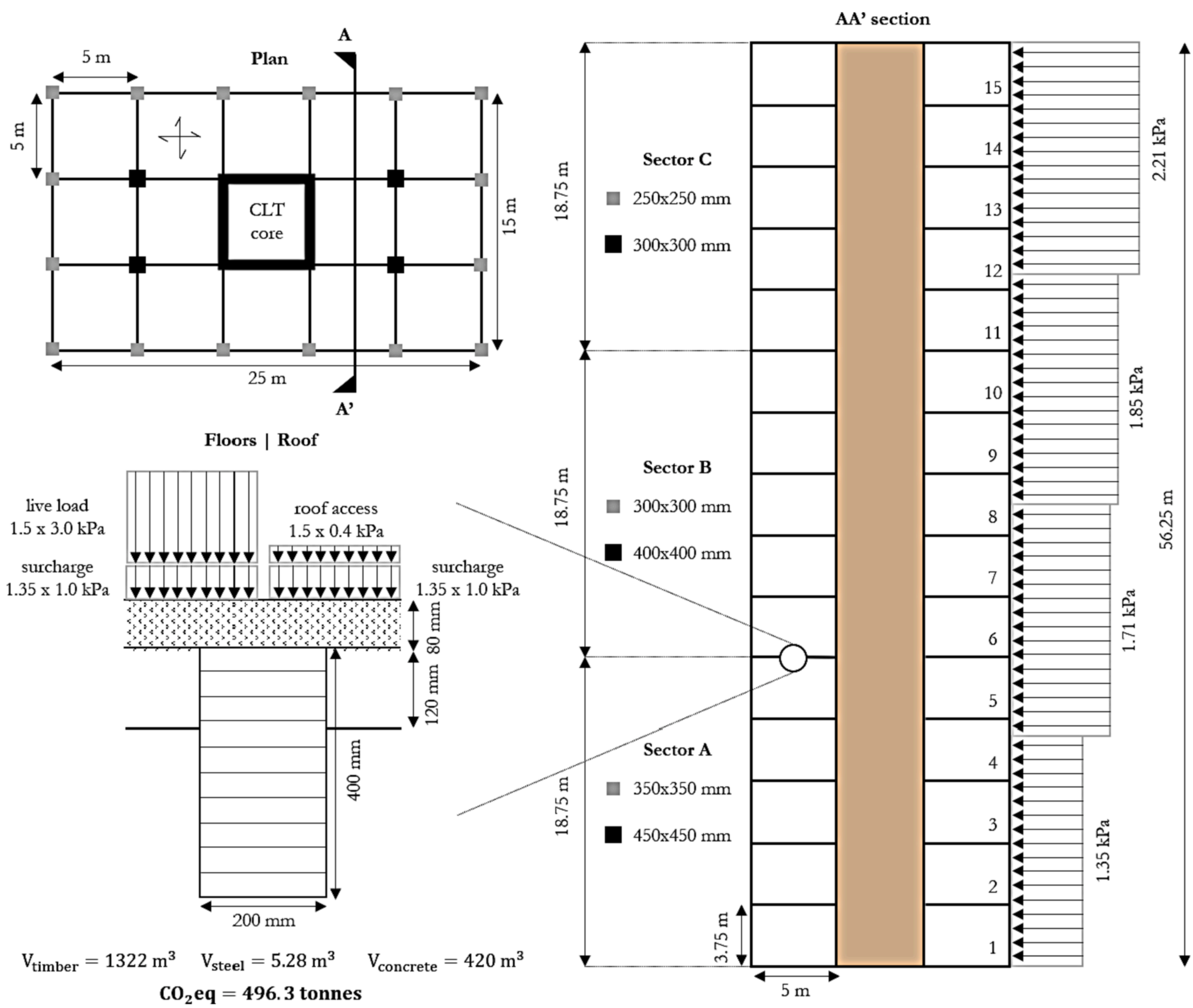

Fig. 6. Case study building primary components, loads, and material tonnage.

3.1.1. Primary components

The building is split into three vertical sectors of decreasing column cross section for material savings. The main features are shown in Fig. 6 and the material properties used in the design in Fig. 7. The building is assumed to be an office (category B) loaded according to the Swiss building code SIA 261 [49] with the timber functioning in service class 1 (dry) according to the Swiss timber building code SIA 265 [50]. The member sizing includes fire design, buckling checks, deflection limits, and long-term effects (creep). Utilisations of members are in the 70–100% range. Floor and roof slabs are assumed to be timber-concrete composites, sized according to the research of Müller and Frangi (2021) [51]. Ongoing innovative research by Kreis (2021) [52] is looking into the possibilities for two-way spanning slabs. For this case study, the slabs are assumed to be two-way spanning without an explicit design, with their serviceability requirements satisfied (deflections, vibrations). Their axial stiffness is taken as the average between timber and concrete, while their in-plane shear stiffness is reduced by a factor equivalent to timber's shear/axial stiffness ratio.

The design has not been focused on horizontal effects as it is assumed that the central core (not explicitly designed) acts like a vertical cantilever and satisfies the ultimate and serviceability limit states. Lateral design in Switzerland is wind-dominated, therefore wind loads have been estimated according to SIA 261 [49] to ensure that floor-floor connections are strong enough to enable the diaphragm action required to transfer the loads to the core. These connections are also providing continuity between the simply supported, single span slabs. All beam and column connections are assumed to be pinned. The substructure has not been designed.

3.1.2. Connection design

While connections are assumed to be pinned in the conceptual design, their actual stiffness and strength have been analytically estimated for all degrees of freedom. This was done using individual connector resistances calculated with the Swiss building codes and assembled analytically as shown in the figures below. Where the Swiss codes could not provide details, such as in the axial withdrawal stiffness of screws, additional help was sought from the Eurocodes and other technical documents referenced below.

The connection behaviour per degree of freedom is simplified to the idealised elastic–plastic curve in Fig. 8. Each of the six curves can be defined with only its elastic stiffness (K_e), yield load (F_y), plastic deformation (δ_p), and ultimate load (F_u). Dowel slip is neglected. Symmetry is assumed in the negative direction, unless otherwise stated. Although the behaviour is hysteretic, no pinching or fatigue have been modelled since the collapse analysis is short-term dynamic and not long-term cyclic. The degrees of freedom are assumed to be independent, i.e., no coupling is accounted for. All failure criteria are concentrated in the connections: that is, the strength of each connection is set as the minimum of the connection and connecting members' strengths.

All properties have been calculated in their design values, however the mean values have been used for the model. In the absence of design-to-mean value expressions, a factor of 1.2 has been applied to estimate the characteristic values, and another factor of 1.2 to estimate the mean values. These factors are determined on average over a number of design calculations without reduction factors, and assuming characteristic resistance values are 5th percentile values following a lognormal distribution with coefficient of variation of 15% (in line with timber resistance probabilistic properties in part 3.05 of the JCSS code [54]).

3.1.3. Beam-Column connection

The Beam-Column (BC) connection is a timber connection with two slotted-in steel plates and steel dowels, fastened to the column with large

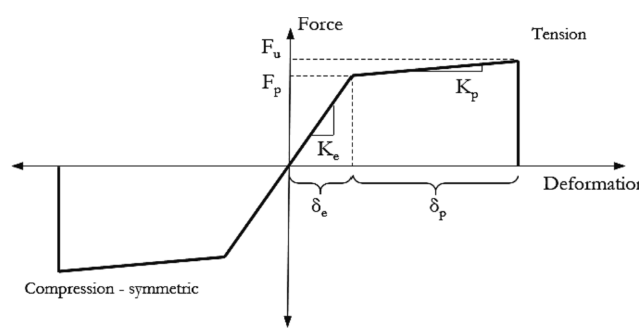

Fig. 8. Idealised elastic–plastic connection behaviour as assumed in the model for each degree of freedom.

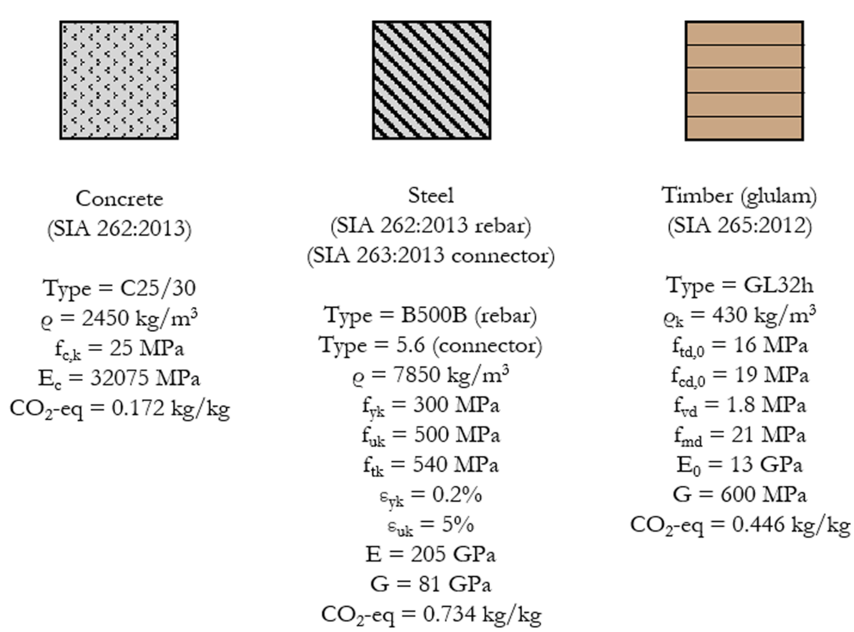

Fig. 7. Material properties and their source reference. Carbon dioxide equivalent values taken from KBOB [53].

screws as shown in Fig. 9. Minimum distances according to SIA265 [50] have been respected. The stiffness and the resistances for all degrees of freedom can be found in the Appendix.

The constituent parts that contribute to the final connection properties are the shear and withdrawal behaviour of the screws, and the shear behaviour of the dowels. The steel plates are assumed to be rigid. The Swiss standard for timber construction SIA265 [50] and the European Technical Approval ETA-12/0063 [55] have been used to calculate the stiffness and capacity of the connectors.

The shear behaviour of both screws and dowels is based on the European Yield Model (EYM) from Johansen (1949) [56]. A “mode 2” behaviour is assumed, with a slight ductility $D_s = 1.5$ according to SIA265:2012 part 6.1.2.3. That is, given elastic deformation δ_e, the plastic deformation is given by $\delta_p = (D_s - 1) \times \delta_e$. In the ductile phase slight kinematic hardening has been preferred over perfect plasticity, modelled as a 1% increase of the yield force at failure, i.e. $F_u = 1.01 \times F_y$. The axial withdrawal behaviour of screws is assumed to be brittle, therefore failure happens suddenly at the yield load.

The connection can be broken down to two parts: the stiffness and resistance contribution due to the column plate screwed onto the column (one shear plane), and the two plates dowelled to the beam (four shear planes). It has been designed to avoid brittle failure modes by making the connector ductile shear behaviour dominant (i.e., weaker). Overall stiffness is calculated by a series addition of the column and beam part stiffness, while overall strength is determined by the weakest link. Connector rows or columns are “compressed” into a single connector of equivalent area for simplification. Axial and shear forces are assumed to be distributed equally in all connectors as shown in Fig. 10 and Fig. 11.

When torsion and bending resistances are calculated, yielding is assumed to happen when the outermost dowel yields (rotation angle θ_y), and failure when the outmost dowel fails (rotation angle θ_u). The overall rotation at yielding and at failure determines the elastic and plastic stiffness respectively. Torsion depends on the shear resistance of the screws only, since the beam steel plates are assumed rigid.

The bending behaviour assumes that the column plate rotates about the outermost column or row of screws. The dowels on the beam side are contributing to the major axis bending resistance like in the torsion case, and in the minor axis bending case they are assumed to all fail as shown in Fig. 13.

3.1.4. Column-Column connection.

Since end grain screws are not accounted for in the Swiss codes, and additional ductility in the column axial direction was sought, the Column-Column (CC) connection has been designed with glued-in rods (GIRs) as shown in Fig. 15 according to the CEN TC 250 (N2579) proposal for the new Eurocode 5 [57]. Minimum distances according to the proposal have been respected. The stiffness and the resistances for all degrees of freedom can be found in the Appendix.

The constituent parts that contribute to the final connection properties are the shear and withdrawal behaviour of individual glued-in rods. Shear is assumed to be slightly ductile, similar to the screws and dowels ($D_s = 1.5$, kinematic hardening 1%), provided that the tensile resistance of the rod, $F_{ax,rod,Rd}$ is at least 1.5 times the bond line resistance, $F_{ax,b,Rd}$. The axial direction is assumed to be quasi-rigid, where the stiffness can be calculated based on the glue shear strength. The steel plates are assumed to be rigid.

Given the symmetry of the connection, the overall stiffness is half the stiffness of each side (series addition of the two identical parts), while the overall strength is the strength of one side only. The overall resistance of the connection is calculated in the same manner as the column part of the BC connection in Fig. 10 (axial and shear resistance), Fig. 12 (torsional resistance) and Fig. 14 (bending resistance).

3.1.5. Floor-Beam & Floor-Floor connections

The overall connection of floors has been designed to be sufficiently strong to transfer wind loads to the core in diaphragm action, which is achieved with the resistance of steel brackets connecting the timber underside of the slabs with the beams (Floor-Beam, FB) and the resistance of concrete rebar embedded into grout (Floor-Floor, FF) directly connecting the floors together. For the former, the “Titan V” bracket from Rothoblaas is used with a full screw pattern according to the European Technical Assessment ETA-11/0496 [58] and the company’s technical sheet [59]. For the latter, the grout is assumed to have the same properties as the C25/30 concrete and axial/shear resistances are calculated using part 6 of the FIB Model Code [60], using only rebar resistances assuming the concrete is cracked.

The in-plane axes (1 & 3) are assumed to be symmetric at the global scale (that is, the entire floor with connectors on all four sides is assumed to have equal resistance on average from all sides). The negative (compressive) in-plane direction is assumed to be rigid due to bearing of the floor slab on the beam sides. Neither connection is modelled to carry bending moments: push–pull pairs along the sides of the slabs activate these (see Fig. 16).

The capacity of the angle brackets in the FB connection has been corrected to its design value by multiplying with load duration and material factors like in the CC connection. For the plastic region, the results from the tests shown in the Rothoblaas technical sheet [59] indicate an average $D_s = 1.5$, which has been used for both in-plane and out-of-plane directions, with a 1% kinematic hardening similar to the BC connection. See the Appendix for the stiffness and resistance in each degree of freedom.

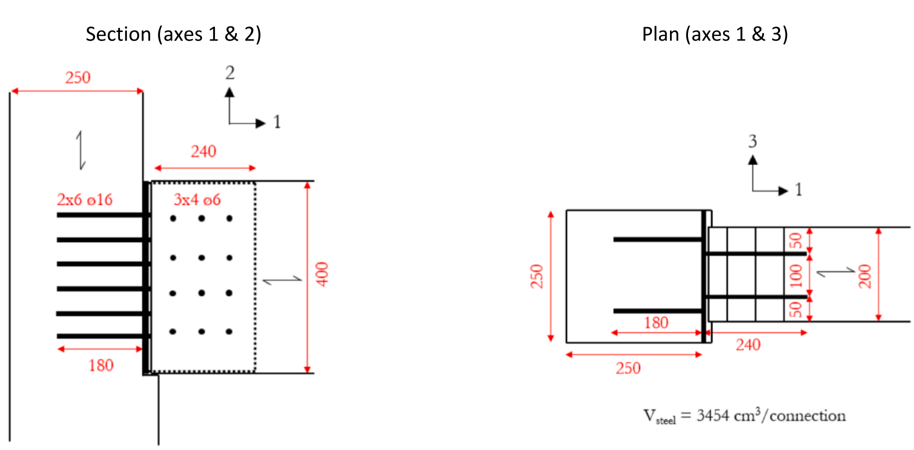

Fig. 9. Beam-Column connection geometry.

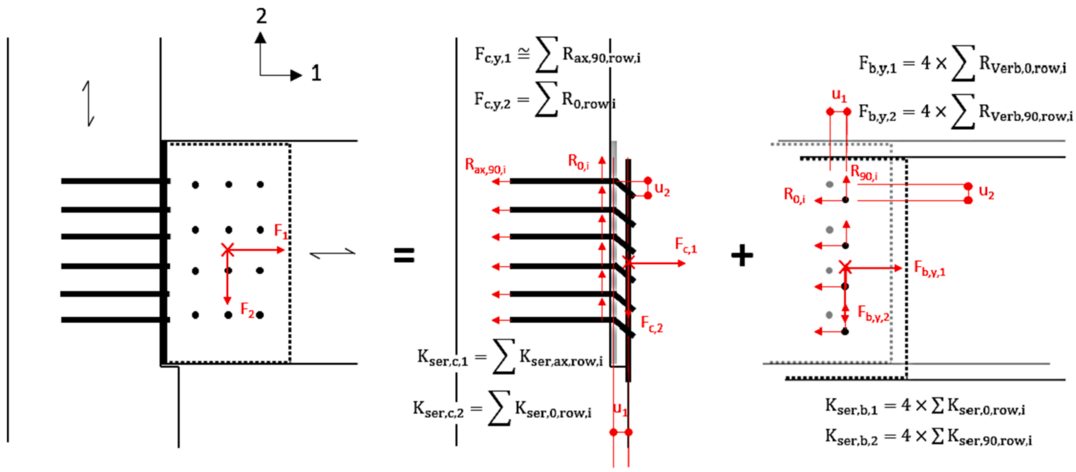

Fig. 10. Beam-Column connection calculation of axial (1) and major axis shear (2) properties.

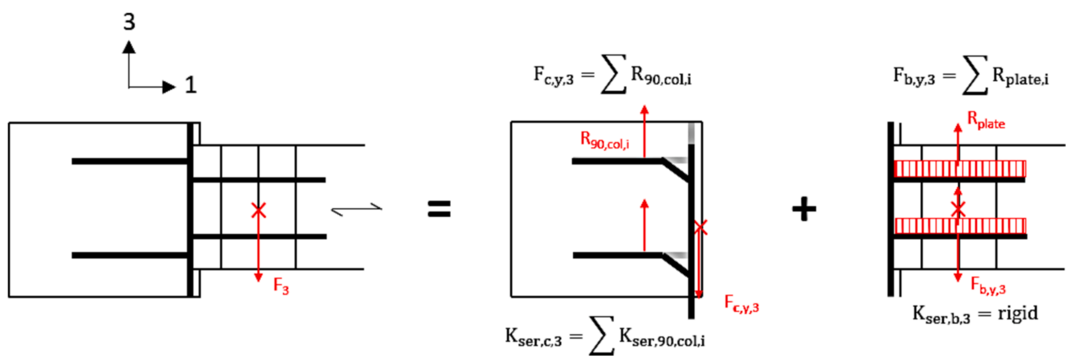

Fig. 11. Beam-Column connection calculation of minor axis shear (3) properties.

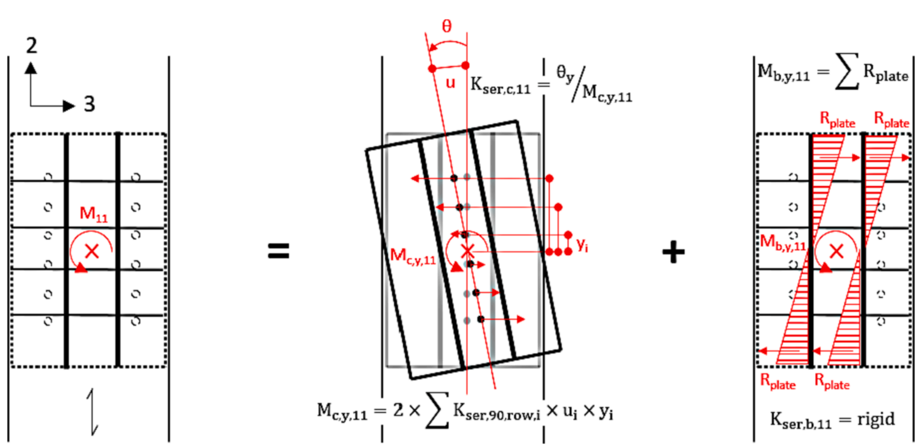

Fig. 12. Beam-Column connection calculation of torsion (11) properties (here shown at the yield point).

3.1.6. Building improvement options

In order to assess the effect of different design options in the robustness performance of the building, four additional building options have been designed and are summarised in Table 1.

The logic behind the choice of the improved options is based on the exploration of: (i) the effect of addressing robustness in different levels of the scale as per Voulpiotis et al. (2021) [2]; and (ii) the importance of connection ductility for robustness as discussed in the literature (see Section 2.2). We therefore chose to examine two design options with "strong floors" from which the remaining floors can be suspended in the case of a column loss in the ground floor, and two design options with ductility improvements in the BC and CC connections. In particular:

- Options 2 & 3 are designed such that the columns can go fully in tension in the weight of the unsupported structure below (maximum half a bay times 14 storeys hanging for option 2 and seven storeys hanging for option 3). One strong floor is placed at the top for option 2 to minimise the architectural impact of the diagonals, while two strong floors are placed at the top and in the middle for option 3 to reduce the required size of the diagonals (fewer hanging floors). For both options the CC connections are much stronger and the columns are larger to accommodate the tensile forces as well as the larger

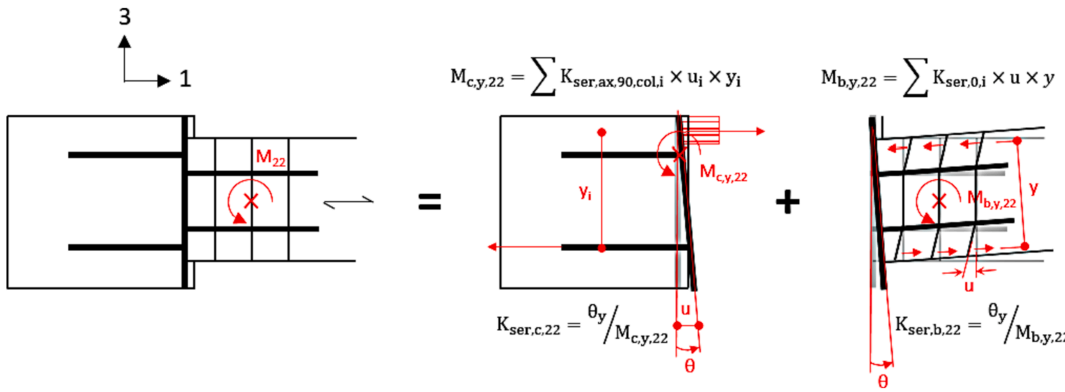

Fig. 13. Beam-Column connection calculation of minor axis bending (22) properties (here shown at the yield point).

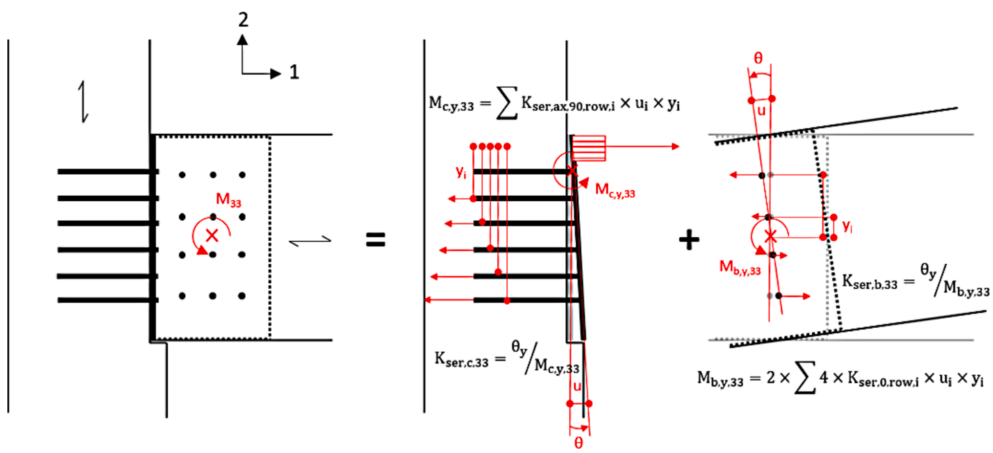

Fig. 14. Beam-Column connection calculation of major axis bending (33) properties (here shown at the yield point).

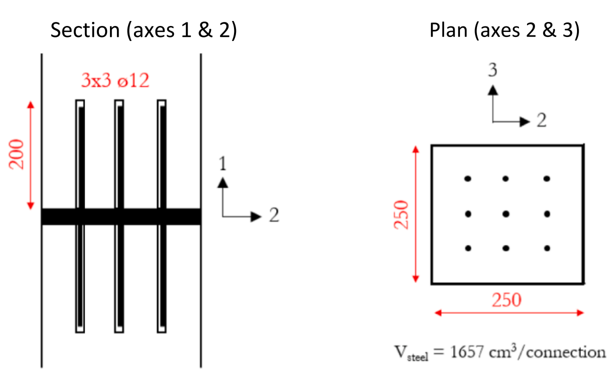

Fig. 15. Column-Column connection geometry.

connections. The truss action required stronger BC connections ("BCS"), designed exactly like the Diagonal-Column connections ("DC"), shown in Fig. 17. The design is similar to the BC connection described previously, with the addition of a back steel plate in the column. As such, the screws are replaced with threaded rods and their withdrawal behaviour is assumed to be rigid and significantly stronger (bearing of the steel plate). It is assumed that the DC connection is also directly connected to the BCS connection via a continuity in the steel plates, such that the large diagonal axial loads do not destroy the column in shear.

- Options 4 & 5 exhibit more ductile connections. In option 4, the BC connection was increased in size to fit 20 dowels instead of twelve, resulting in a strength increase of 76% (average across all degrees of freedom). A ductility of $D_s = 3.0$ was assumed given the small dowel size to connection size ratio. To maintain failure at the dowels, the number of screws to the column also had to be increased, subsequently increasing the size of the columns. The CC connection was changed to a 250 mm long, 8 mm diameter 4x4 glued-in rod pattern, resulting in a slightly weaker connection. In option 5, only the CC connection change was applied, this time assuming the smaller diameter glued-in rods would achieve a ductility with $D_s = 3.0$. This resulted in 23% strength loss.

It should be noted that ductility upgrades were performed with consideration of the accidental load case scenarios analysed in this case study and not according to the earthquake engineering standards and other cyclic loading considerations. In particular, ductile zones did not follow the "strong column, weak beam" theory of earthquake design, nor were the connections adjacent to the regions of increased ductility designed for overstrength to avoid brittle failure. A consideration of these earthquake-related qualities for the improvement of robustness performance is a worthwhile future investment.

3.2. Finite Element model setup

3.2.1. Abaqus® model

The numerical implementation of the model was done in Simulia's Abaqus® 2021 software [61]. Both implicit (Abaqus/Standard) and explicit (Abaqus/Explicit) solvers have been used in the analysis. The former is an excellent solver for smooth model responses, like static or dynamic nonlinear analyses without material failure (the undamaged state analysis in this case study), while the latter is a suitable option

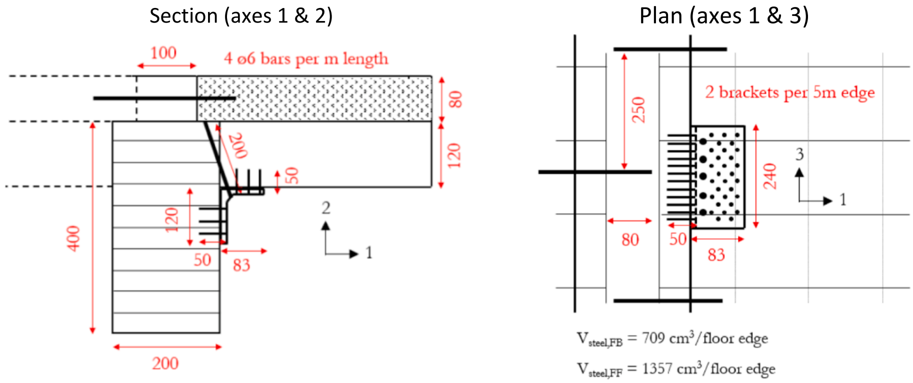

Fig. 16. Floor-Beam and Floor-Floor connection geometry.

Table 1
Design improvements summarised. Full details and drawings are given in the Appendix.

#	Improvement description	V_{timber} (m^3)	V_{steel} (m^3)	$V_{concrete}$ (m^3)	CO_2-eq (t)
1	Design as per Section 3.1	1322	5.28	420	496.3
2	Floor 15 is a diagonal-braced strong floor. CC connection is 232% stronger	1383 (+4.6%)	7.03 (+33.1%)	420 (+0.0%)	519.6 (+4.7%)
3	Floors 7 & 15 are diagonal-braced strong floors. CC connection is 94% stronger	1380 (+4.4%)	7.34 (+39.0%)	420 (+0.0%)	520.8 (+5.0%)
4	BC connection is 76% stronger and twice as ductile. CC connection is 23% weaker	1330 (+0.6%)	7.35 (+39.2%)	420 (+0.0%)	510.0 (+2.8%)
5	CC connection is twice as ductile but 23% weaker	1322 (+0.0%)	5.276 (-0.02%)	420 (+0.0%)	469.27 (-0.002%)

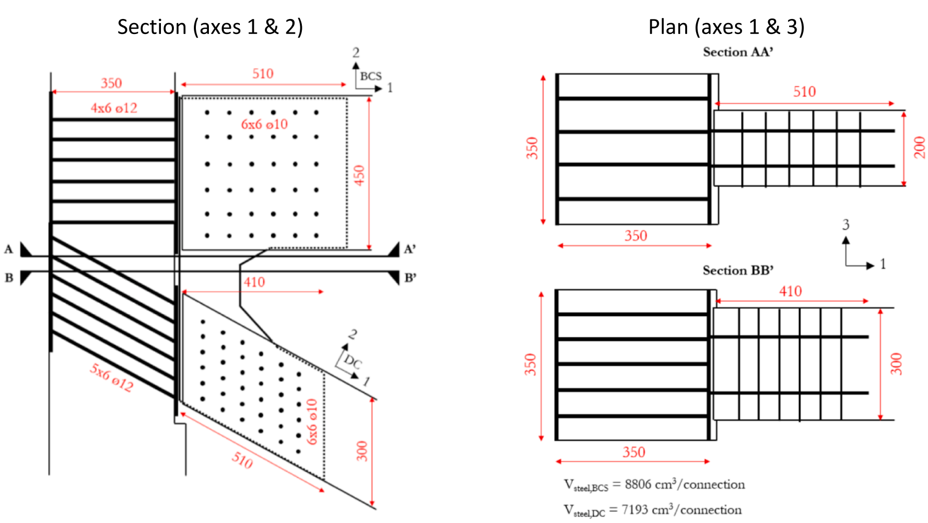

Fig. 17. Beam-Column (strong) and Diagonal-Column connection geometry.

when the response is non-smooth, like in dynamic analyses where convergence of the implicit solver is difficult or impossible due to contacts and element failures (the collapse analysis in this case study) [62].

The model setup is shown in Fig. 19. The choices of elements are the simplest possible while sufficing for the explicit solver analysis and expected large deformations. The loads are applied via density only, in order to be included in the eigenfrequency analyses to calculate damping coefficients if needed. Element contact is introduced in vertical slab pairs to model debris loading and allow the possibility of pancake collapse. The choice of "soft" contact behaviour (finite normal and tangential contact stiffness) was only to avoid potential numerical instabilities. The connectors are modelled as wires of finite length to account for the connection eccentricities. The behaviour is introduced as idealised elastic–plastic with failure (Fig. 8). The column removal is introduced by lowering its stiffness with the application of a temperature field. This way only that member is softening in the model, while the connections at its ends remain intact.

A rather coarse mesh has been chosen for the analysis (1/4th of the

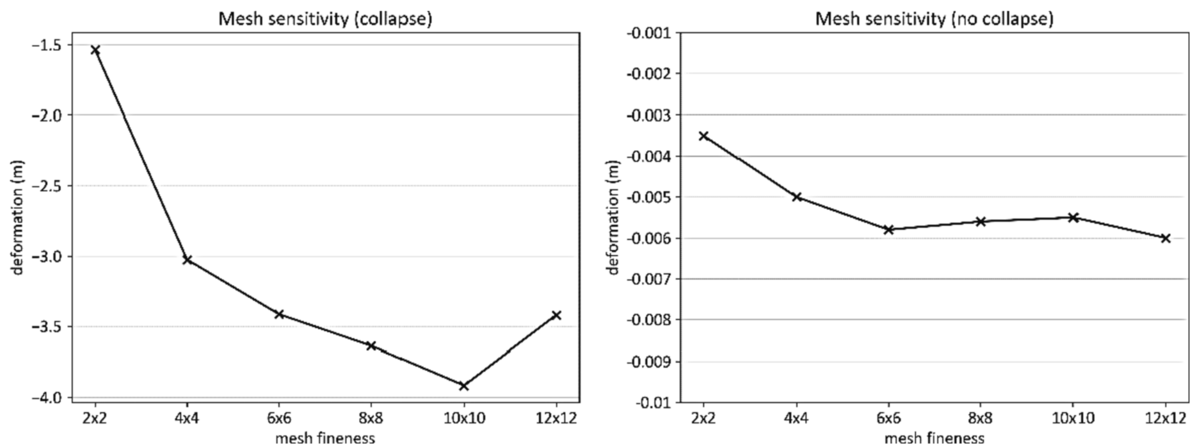

Fig. 18. Sensitivity of the model deformation at two selected points (collapsed and not collapsed floor) to the mesh fineness.

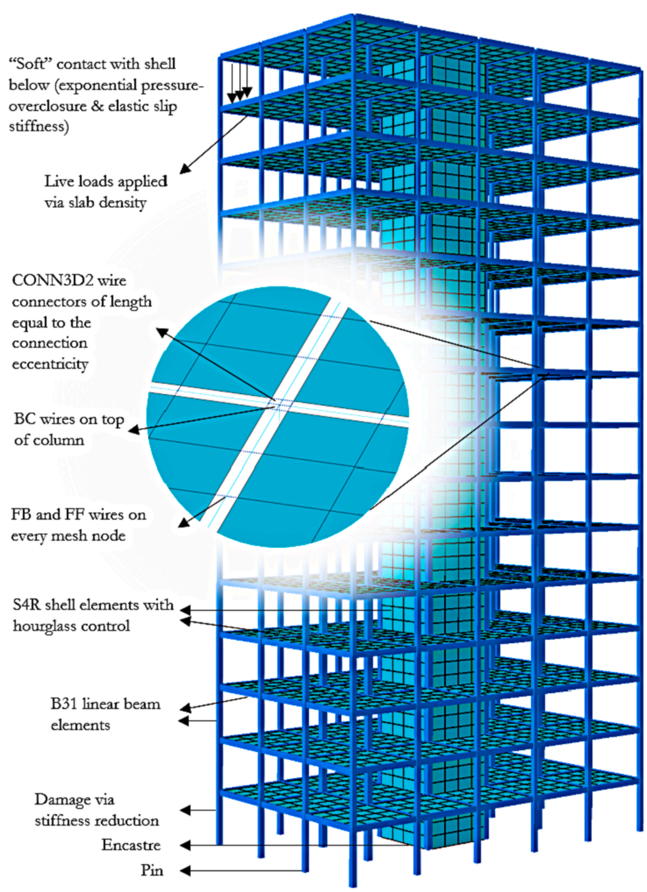

Fig. 19. Model setup in Abaqus.

bay size) following a sensitivity study to find the balance between accuracy and solver speed, the latter being a priority (Fig. 18).

3.2.2. Model validation

The robustness quantification results never depend on the output of a single model: rather, they stem out of model comparison, such that errors or inaccuracies cancel out. Two additional checks have been carried out in the model itself to validate the results further:

- The exact same analysis procedure used for the whole building in Abaqus has been tested in a timber beam carrying a uniformly distributed load, spanning between two simple supports and propped by a supporting column. A static analysis is first carried out in Abaqus/Standard to calculate the service stresses and deformations. In a second step (Abaqus/Explicit), the column support is suddenly removed and the beam is let to oscillate. The removal is causing the beam span to double and the midspan stresses to dynamically increase. The model stresses and deformations were calculated analytically using beam formulas [63] and assuming a Dynamic Amplification Factor of 2.0 according to Cao et al. (2021) [29]. A deviation of less than 4% was found between the analytical and the numerical calculations, proving the validity of the complex two-step, implicit-explicit Abaqus process to model structures suddenly damaged while in service.
- The full model output stability has been checked for slight variations of the failure criteria. In particular, the floor deformations of the original design at 1.3 and 2.6 s after the onset of damage have been plotted for a $\pm$ 2% variation of the BC connection ductility, $D_{s,BC}$ (Fig. 20). The model outputs at 2.6 s show a chaotic behaviour, i.e. small variations in the failure criteria of the model lead to large variations of the output. The model outputs at 1.3 s are mostly stable. The same pattern is observed when $f_{u,BC}$ and ρ_{beam} are varied. The 1.3 s timestamp was the last analysis frame with acceptable stability and therefore all model results are extracted from this time interval (the 2.6 s was only to demonstrate the chaotic behaviour). The model is therefore only following the development of the first alternative load paths and collapse arrest (if any), or the first few stages of collapse propagation. Models which try to follow the entire collapse progression, like the one presented by Domaneschi et al. (2020) [64], are usually fully calibrated to actual collapse data from experiments or real situations. Without such data, modelling a full collapse from start to finish will include a lot of chaos and guesswork.

3.2.3. Damage scenarios

Each design option has been studied against disproportionate collapse in three separate damage scenarios shown in Fig. 21, with their equivalent direct failure areas assumed to be circular of radius half the bay span (i.e., $r = 2.5\text{m}$). The scenarios cover both external and internal damage and are assumed to be equiprobable. The removal speed is $t_{removal} = 2\,\text{ms}$, corresponding to a sudden failure (for example, due to explosion). Using a collapse criterion $\delta_{crit} = 1.5\,\text{m}$, the collapse flag matrices and total failure area (collapse severity) were calculated according to Section 2.

3.3. Collapse classification

3.3.1. Probabilistic model summary

To minimise the model dimensionality and yet sufficiently explore the factors that lead to collapse, we kept all geometrical aspects constant

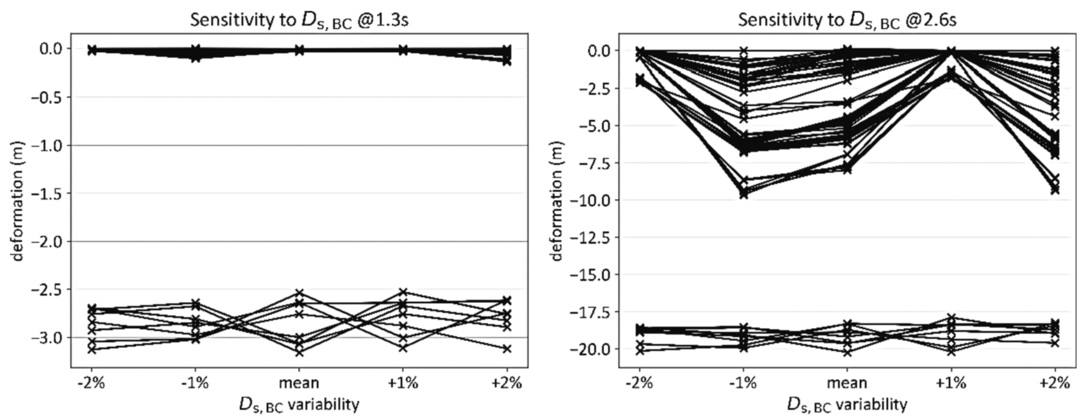

Fig. 20. Model stability check by varying the ductility of the BC connection by ±2% (scenario 1, damage scenario 1).

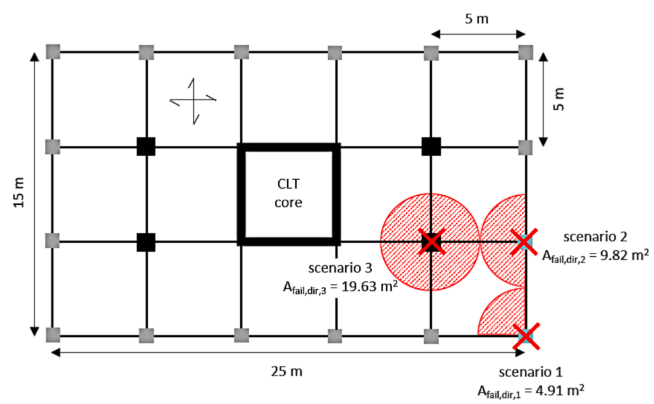

Fig. 21. Summary of damage scenarios and their equivalent direct failure areas (ground floor).

(bay sizes, storey height, component lengths and thicknesses, et cetera) and varied the timber density, timber modulus of elasticity, steel ultimate strength, and connection ductility ratios. We made this choice since these probabilistic variables are the starting point for all the connection properties, where all the failure criteria are concentrated. The recommendations of the Joint Committee for Structural Safety (JCSS) for steel and timber have been used [54], although ongoing research is suggesting slightly different distributions and coefficients of variation [65], which are worth exploring in the future. The probabilistic definition of the live load is rather complicated, therefore a simplified approach using a Gumbel max distribution is used. All the inputs are assumed to be independent, i.e. no copula is defined in the input space. A summary of all variables is shown in Table 2.

Table 2
Probabilistic variables (input vector) for the base design of the case study building.

Variable	Mean	CoV	Distribution	Reference
Live load (q)	1.8 kPa	22%	Gumbel max	Fahrni (2021) [66]
$E_{0,beam}$	13 GPa	13%	Lognormal	JCSS 3.5.3.2
$E_{0,column}$	13 GPa	13%	Lognormal	JCSS 3.5.3.2
$E_{0,floor.av}$	21 GPa	13%	Lognormal	JCSS 3.5.3.2
ρ_{beam}	490 kg/m^3	10%	Normal	JCSS 3.5.3.2
ρ_{column}	490 kg/m^3	10%	Normal	JCSS 3.5.3.2
$\rho_{floor,timber}$	490 kg/m^3	10%	Normal	JCSS 3.5.3.2
$f_{u,BC}$	500 MPa	4%	Lognormal	JCSS 3.2
$f_{u,CC}$	500 MPa	4%	Lognormal	JCSS 3.2
$D_{s,BC}$	1.5	1–2 (bounds)	Uniform	Assumption
$D_{s,CC}$	1.5	1–2 (bounds)	Uniform	Assumption
$D_{s,FB}$	1.5	1–2 (bounds)	Uniform	Assumption

3.3.2. Random Forest classifier

To calculate the probability of occurrence of each collapse class, we chose the Random Forest (RF) classifier for its versatility, speed, and interpretability. We will not cover the details of the Random Forest in the main body of this paper, the reader can refer to the Appendix for details on how we chose this classifier and optimised the hyper-parameters using a randomised search grid. Full details can be found in Breiman (2001) [67]. To address the class imbalance problem (accuracy loss in rare collapse classes), we used the popular "Synthetic Minority Oversampling TEchnique" (SMOTE) to oversample in the input domain of these classes. This algorithm creates new input samples between an existing sample of the minority class and its neighbours. The details of the method are described in Chawla et al. (2002) [68] and are implemented in the model with the "imbalanced-learn" Python module [69].

3.3.3. Performance scores

We measured the performance of the classifier by obtaining the accuracy scores using k-fold cross-validation according to Kohavi (1995) [70]. The training data is split into k number of "folds" (or simply sets) and the classifier is trained k times in (k −1) folds, using the left-out fold each time to validate the performance. Both the accuracy and macro-f1 (insensitive to class imbalance) scores have been used in this research. More details can be found in the scikit-learn website [71].

3.3.4. Sensitivity study

It is essential to measure the contribution of each probabilistic input parameter to the model output such that we can decide where (not) to focus our resources in future research or design situations. We decided to use the Impurity-Based Importance (IBI) measure since it is an analytical by-product of the Random Forest classifier: when the information gain at a decision tree split due to an input variable is large, this variable is considered important. Full details are provided in Scornet (2020) [72].

4. Results & discussion

Disclaimer: These results are unique to the case study building designed for this research and cannot be used to draw conclusions about all tall timber buildings, even if they are similarly designed.

All analyses were run on the "Euler" High Performance Computer of ETH Zürich [73]. Using master scripts in Python and a batching system, Abaqus input files and job submissions were performed in parallel by both Intel® and AMD® compute nodes. With a different python script, a Random Forest classifier for each design option and damage scenario was set up using the module "scikit-learn" according to Section 3.3.

For each design option and damage scenario, a random set of 10,000 samples of the input vector was initially generated to train the classifier with the collapse severity ($A_{Fail,Ind}$) as the output. Each design option was run until at least 1,000 models were solved for each scenario. This took on average 2–3 weeks of computation when running 15 models in parallel (limited by the software licensing fair usage), each of which used five cores with 20 GB assigned memory. An input pool of one million random samples of the input vector was also generated to sufficiently capture the probabilistic input space. These were used to calculate the robustness indices using the trained classifier.

Results were then post-processed to identify rare collapse classes and assemble new input vectors using SMOTE according to Section 3.3.2. A second round of simulations for each design option enriched the classifier with at least 300 new minority samples.

4.1. Detailed results

Please refer to the Appendix for the detailed histograms of the collapse extent for each design option and damage scenario.

The code-compliant design option 1 partially collapses in all three damage scenarios. Additionally, a dominant collapse class is always present (375 m^2 for scenario 1; 1,100 m^2 for scenario 2; and 2,200 m^2 for scenario 3, see Fig. 22). The extent of the collapse is increasingly worse by scenario: a corner column removal causes the entire corner of the building to collapse, an edge column removal causes the entire edge of the building to collapse, and an internal column removal causes half the building to collapse (until the assumed rigid core).

The mechanics of the collapses in design option 1 are simple to explain by scenario:

Scenario 1: The load of the 14 unsupported floors is initially transferred towards the neighbouring columns via the beams in cantilever action, and via the floors in in-plane shear action. The BC and FB connections break very quickly, and the entire corner of the building, with the floor slabs detached, is accelerating towards the ground.

Scenario 2: The mechanism is similar to scenario 1, however this time the unsupported area is double in size and the forces carried by three beams and two slabs per storey. The horizontal forces developing in the edge beams pull on the adjacent corner column, causing it to buckle and collapse too.

Scenario 3: With an even larger initial failure (four times that of scenario 1), a larger portion of the internal frame spreads loads to its surrounding beams and slabs in the same manner with scenarios 1 & 2. However, horizontal resistance is only provided from one side, the core, causing everything on the outer side of the building to buckle and collapse as well.

No collapse was observed for damage scenario 1 in design option 2, where the top floor is a trussed “strong floor”. Although to a significantly lesser extent than in design option 1, the failure of an edge or an internal column again caused a progressive collapse.

The collapses and how they were caused are shown in Fig. 23. The truss structure is unable to carry the weight of the unsupported building when its area exceeds half a bay. It is therefore not surprising that scenario 3 leads to a collapse, albeit of lower initial extent than in the original design option. Upon removal of the column, the CC connection breaks axially, and the membrane action that develops in the slabs is pulling the surrounding structure inward. Since stiffness is asymmetric (the core side is much stiffer), the edge of the building buckles and a substantial collapse initiates.

Scenario 2 is more marginal in that it could have supported the weight of the collapsing building had dynamic factors been included in the sizing of the stronger connections. However, the design of the strong floor was static, and the fast column removal speed is causing larger, dynamic force reactions. The failure that caused the collapse was the CC connection in shear at the floor below the truss. This indicates that the strong floor is not stiff enough to prevent large deformations that will induce very large forces in the surrounding connections. Also, even the much stronger CC connections are not particularly strong in shear: an alternative for this degree of freedom is an option worth exploring.

Design option 3 was similar to design option 2 in that scenario 1 was fully arrested. Scenario 2, however, showed a wider and more severe response spectrum (severities up to 1,300 m^2 compared to 950 m^2 for design option 2). Looking at the mechanics of the collapse a bit more closely (Fig. 24), we see that for the worst collapse class (1,300 m^2), shear failure both above and below the truss strong floor in the middle of the building is destabilising the edge of the building. Collapse very quickly spreads to the lower half.

Scenario 3 shows mixed results: in most cases the building survived. No axial failure at the column connections was observed. There were, however, cases where again the shear failure of the CC connection under the middle strong floor caused the initially contained collapse to spread downward. Unlike design option 1, the horizontal connectivity with the truss reduced the initial spread of the damage to the adjacent corner column in both design options 2 & 3.

Design option 4 did not, on average, show collapse resistance improvement: although scenario 1 sometimes survived the damage, the spread of collapse classes was much wider with the majority collapse

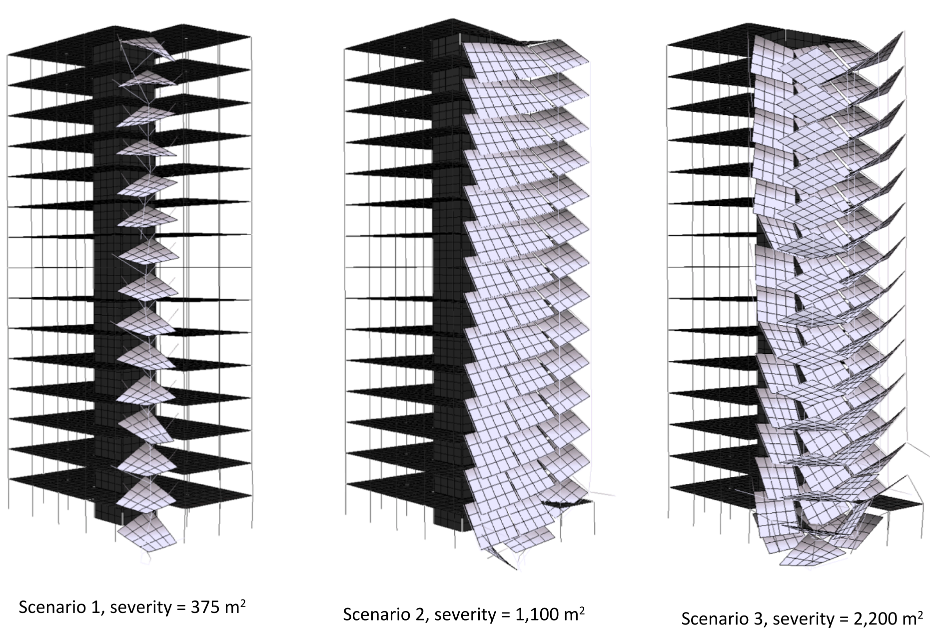

Fig. 22. Collapse images extracted from Abaqus for the dominant collapse classes of design option 1.

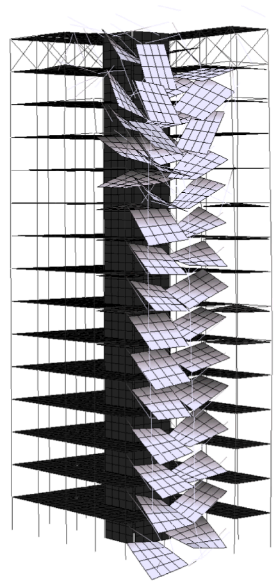

Scenario 2 @1.3 s, severity = 850 m^2

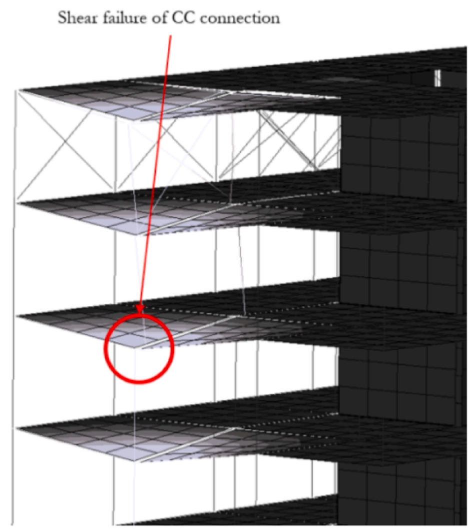

Scenario 2 @0.4 s, column connection shear failure

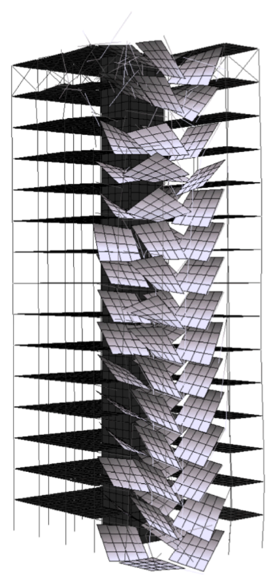

Scenario 3 @1.3 s, severity = 1,200 m^2

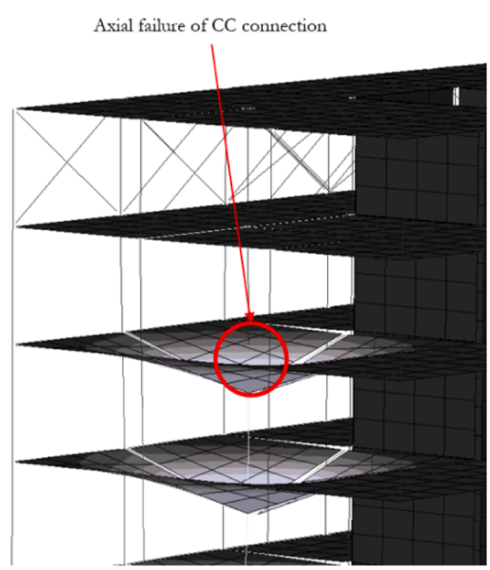

Scenario 3 @0.5 s, column connection axial failure

Fig. 23. Collapse images extracted from Abaqus for design option 2.

class still being the corner bay as with design option 1, with similar mechanics described earlier and shown in Fig. 22. Damage scenarios 2 & 3 showed very consistent behaviour despite the variability of the probabilistic inputs. A possible explanation is that although alternative load paths changed with the improved connections, they could not find their way back to the core. A closer look at the simultaneous improvement of the floor slab design and connectivity, together with the beam and column connectivity, is a worthwhile investment.

Finally, in design option 5, the small change of the CC connection to increase its ductility did not improve the robustness performance at all. Rather, its reduced strength made matters slightly worse than in the original design option. Collapse mechanics were also similar to option 1, shown in Fig. 22.

4.2. Robustness indices

The table of all robustness indices and performance indicators is presented below. The classifier accuracy and f1 scores are provided underneath each robustness index (see Table 3).

With a 34-fold increase in the average robustness index ($AGR = 34$), design options 2 & 3 with structural improvements in the whole building scale (“strong floors”) are much better solutions for this particular building. They owe this improvement due to the full arrest of collapse in scenario 1 ($I_{Rob,sc1} = 1.0$) and the marginal, but insufficient improvement of collapse in scenarios 2 and 3 ($I_{Rob,sc2/3} < 0.03$, which is practically not different to zero). For architectural reasons one could argue that having only one “strong floor” is preferable and thus option 2 would be the best despite its marginally lower score. This result is in line with the observations of Mpidi Bita et al. (2019) [20], who also proved the

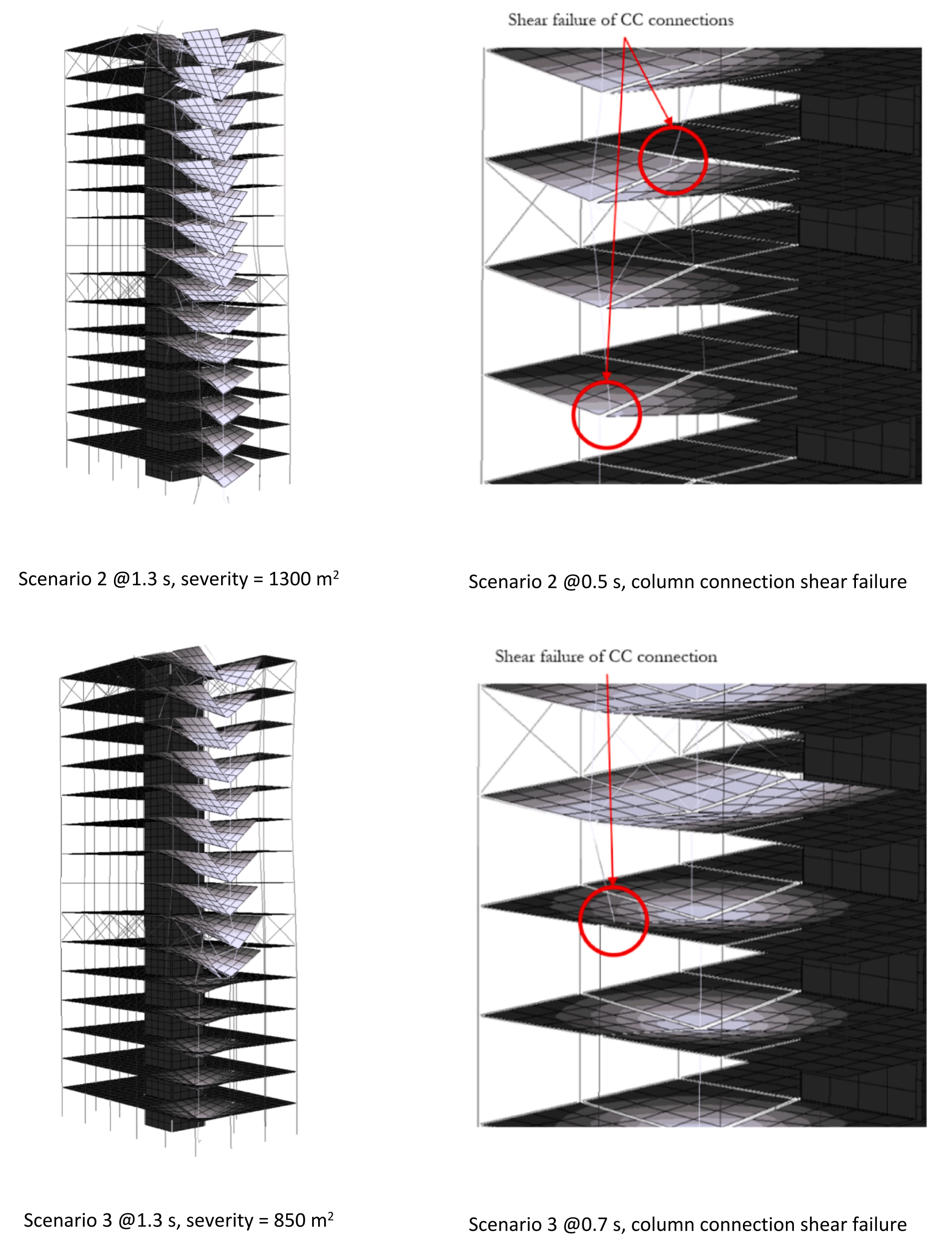

Fig. 24. Collapse images extracted from Abaqus for design option 3.

benefit of designing a strong floor from which columns can hang the floors below in case of damage. The benefit of the conceptual design is evident despite their study being on a different structural typology (flat-plate CLT building). Design option 4, equally robust as option 1, requires more steel in the connections and thus becomes uneconomic in the given assumptions. This is not to say that an improvement in the connections cannot increase robustness; rather, the specific solution implemented does not provide sufficient alternative load paths. Design option 5 is marginally worse than the starting option in terms of performance. These results are in line with the alternative load paths and collapse mechanisms discussed in Section 4.1. They highlight once again the significance of understanding how alternative load paths are formed, and making sure they lead to the ground. Increasing the ductility of only two connections (e.g. BC and CC in option 4) allows loads to better redistribute in these parts of the structure, however collapse resistance is also dependent on the FB and FF connections, global stiffness symmetry, and the buckling of columns. One should have a clear understanding of the flow of loads in a structure at the global scale (conceptual design) in order to make the right decisions regarding connection and component detailing.

4.3. Sensitivity study results

The five most important inputs according to the Impurity-Based Importance (see Section 3.3.4) are shown in Fig. 25.

The properties of the columns and the Column-Column connections dominate the importance for external damage (scenarios 1 & 2), while the properties of the beams and floors dominate the importance for internal damage (scenario 3). However, the spread of importance values throughout the Random Forest is high (wide vertical groups of circles), and the importance values themselves are neither high, nor very different to each other. This indicates an absence of an overall dominant feature, which reflects the observations in Sections 4.1 and 4.2, and explains why design options 4 & 5 do not perform better in terms of robustness. Collapse is arrested by the structure functioning as a large, complex system and an improvement on many variables, rather than just

Table 3
The "Magic Table" of robustness comparison between all the design options (with ac/f1 scores).

	$I_{Rob,sc1}$	$I_{Rob,sc2}$	$I_{Rob,sc3}$	$I_{Rob(av)}$	CO_2eq (t)	AGR[1]
Concept 1 scores	0.0129 (0.94 / 0.75)	0.0088 (0.73 / 0.40)	0.0088 (0.90 / 0.63)	**0.010**	**496.3**	**1**
Concept 2 scores	1.00 (0.83 / 0.36)	0.0182 (0.58 / 0.46)	0.0144 (0.76 / 0.71)	**0.344**	**519.6** (+4.7%)	**34**
Concept 3 scores	1.00 (1.00 / 1.00)	0.0133 (0.56 / 0.43)	0.0274 (0.70 / 0.49)	**0.347**	**520.8** (+5.0%)	**34**
Concept 4 scores	0.0119 (0.68 / 0.49)	0.0091 (1.00 / 1.00)	0.0090 (1.00 / 1.00)	**0.010**	**505.4** (+2.4%)	**1**
Concept 5 scores	0.0095 (0.69 / 0.63)	0.0059 (0.33 / 0.33)	0.0088 (1.00 / 1.00)	**0.008**	**496.27** (-0.002%)	**0.8**
Average	0.4069	0.0110	0.0137			
$W_{scen,i}$	1/3	1/3	1/3			
$A_{Fail,Dir}$	4.91	9.82	19.63			

[1]Absolute Geometry Rating according to Voulpiotis et al. (2021) [2], equal to the ratio of the average robustness index of the option in question, to the average robustness index of the starting option.

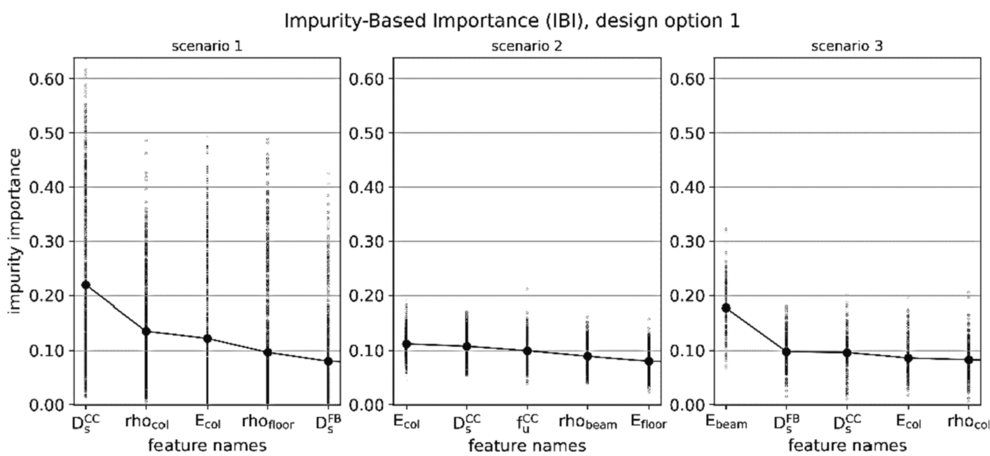

Fig. 25. Impurity-based importance (IBI) for the five most important inputs in design option 1.

a few, is necessary to achieve an overall better robustness performance.

A comparison of the sensitivity study between different design options is shown in the Appendix.

4.4. Model limitations & suggested improvements

Self-criticism on the methods used is as important as the research itself. An overview of the strengths and limitations of each section is presented in Table 4.

The most important improvements shall be in the model definition: accurate, coupled connection properties should be determined by an experimental campaign; the floor slab in-plane shear behaviour shall be modelled in more detail; and structural damping shall be included by (i) implementing an iterative damping scheme where the changes in the mass and tangent stiffness of the model change the damping as the collapse progresses; (ii) estimating the damping parameters for each of the structural elements and connections; (iii) implementing a more appropriate global damping formulation such as uniform or modal damping; and (iv) implementing a hybrid damping formulation accounting for both local and global damping.

The numerical modelling approach (nonlinear dynamic FEM) is rather advanced, although there exist other methods that may be more suitable alone or in combination with this FEM approach. In particular, the Applied Element Method (AEM), as described in Kiakojouri et al. (2020) [74], has the crucial benefit of being able to improve model element separation, making it more suitable for modelling failure and collapse. That said, the software, support, and experience available for the AEM is very limited compared to the FEM, and the validity of the results has not been checked as much as in the FEM. Ultimately, validation of the models should be accompanied by experiments.

The classification can be upgraded with Active Learning: an iterative process in which an initially trained classifier is enriched with samples from areas of interest in the input space (such as close to failure domains), rather than random ones. A state-of-the-art of Active Learning and its potential for use in reliability problems is summarised in Moustapha et al. (2022) [75]. Minority oversampling, which has been used in this research, is also a model enrichment method which can be combined with Active Learning to maximise the learning potential of a small sample set. This is a fascinating ongoing area of research, with worked case study examples presented in Benner et al. (2015) [76] and Kapteyn et al. (2020) [77].

5. Conclusion

The work presented in this paper is an advanced robustness quantification of a tall timber building. The quantification procedure was only made possible by some advanced modelling techniques. In particular:

- We designed an imaginary 15-storey CLT-core, post-and-beam tall timber building and four additional improved versions of it, all

Table 4
Evaluation of all the methods used in this research (with section numbers).

Section	Benefits	Limitations
Building design (3.1)	+ Realistic design for construction + Detailed design of the connections + Parametrically setup such that various options can be studied	− Floor slabs not explicitly designed to span bidirectionally − Connection properties based on conservative building codes
FE model (3.2)	+ Accounts for dynamic effects + All types of nonlinearities are included + Suitable to study entire buildings	− Slow despite the explicit algorithm − Complex and impossible to reproduce with hand calculations − Simplified to 1D and 2D elements − Damping not included
Collapse classifier (3.3)	+ Propagates uncertainty efficiently given only a couple thousand model runs + Outputs sensitivity measures of the input parameters	− Is prone to overfitting − Input vector is random, leading to efficiency loss
Results (4.1 - 4.3)	+ Demonstrate the increase of robustness given structural changes + Valuable insight on collapse mechanics + Valuable insight on the impact of the design parameters to the collapse behaviour	− Cannot be generalised for other buildings − Show chaotic tendencies therefore cannot be used to study full collapse propagation − Resistance to systematic exposures not studied

according to the Swiss building codes. Particular attention was put into calculating the stiffness and strength of all connections in all degrees of freedom.

- The buildings were then analysed using detailed nonlinear dynamic Finite Element models in three ground floor column removal scenarios to calculate the resulting robustness indices and to compare their disproportionate collapse performance.
- The robustness indices were calculated by using a Random Forest classifier. Model enrichment with the Synthetic Minority Oversampling TEchnique (SMOTE) algorithm were used to improve the classifier performance.

The results of the case study show us that:

- Design improvements in the global building scale (trussed "strong floors") seem more effective in preventing disproportionate collapse than increasing the strength and ductility of selected connections.
- Higher order behaviour (e.g. buckling, geometrical nonlinearities, stiffness asymmetries) had a decisive role in the collapse progression.
- Following a sensitivity study with the use of Impurity-Based Importance (IBI), we found that column properties are more important for preventing collapse in external column damage scenarios, while beam and floor properties are more important for preventing collapse in the internal column damage scenario. However, there is a marked absence of a dominant feature: collapse prevention depends on the simultaneous improvement of many design variables.

It is important to determine in more detail and experimentally validate the connection and floor slab behaviour. Moreover, a detailed damping formulation should be considered in the future. Finally, the classification of the model can perform better with Active Learning methods. The full details of the case study are vast and must be understood before these conclusions are employed in practice. Please refer to the doctoral thesis of Voulpiotis (2021) [3] for more details.

This work is contributing to the increasing body of knowledge of disproportionate collapse prevention of tall timber buildings, offering with it a quantification and modelling framework which can be used for any other building. We hope that explicit quantification efforts will continue increasing researchers' and designers' knowledge on how to design tall timber buildings safely.

CRediT authorship contribution statement

Konstantinos Voulpiotis: Conceptualization, Formal analysis, Software, Methodology, Visualization, Writing – original draft, Writing – review & editing. **Styfen Schär:** Formal analysis, Software, Methodology, Writing – review & editing. **Andrea Frangi:** Project administration, Funding acquisition, Writing – review & editing.

Declaration of Competing Interest

The authors declare that they have no known competing financial interests or personal relationships that could have appeared to influence the work reported in this paper.

Acknowledgements

We are thankful for the financial support of the Albert Lück Stiftung which makes this research possible. Special thanks also go to COST Action FP1402 for enabling the collaboration between ETH Zurich and the NTNU in Trondheim.

Appendix A. Supplementary material

Supplementary data to this article can be found online at https://doi.org/10.1016/j.engstruct.2022.114427.

References

[1] Bussell MN, Jones AEK. Robustness and the relevance of ronan point today. Struct Eng 2010;88:20–5.
[2] Voulpiotis K, Köhler J, Jockwer R, Frangi A. A holistic framework for designing for structural robustness in tall timber buildings. Eng Struct 2021;227:111432. https://doi.org/10.1016/j.engstruct.2020.111432.
[3] Voulpiotis K. Robustness of Tall Timber Buildings. Swiss Federal Institute of Technology (ETH); 2021. https://doi.org/10.3929/ethz-b-000526211.
[4] Mpidi BH. Disproportionate collapse prevention analyses for mid-rise cross-laminated timber platform-type buildings. University of British Columbia; 2019.
[5] Byfield M, Mudalige W, Morison C, Stoddart E. A review of progressive collapse research and regulations. Proc Inst Civ Eng - Struct Build 2014;167(8):447–56. https://doi.org/10.1680/stbu.12.00023.

[6] Adam JM, Parisi F, Sagaseta J, Lu X. Research and practice on progressive collapse and robustness of building structures in the 21st century. Eng Struct 2018;173: 122–49. https://doi.org/10.1016/j.engstruct.2018.06.082.

[7] EN 1991-1-7: European Committee for Standardisation (CEN). European Standard - Eurocode 1 — Actions on structures — Part 1-7: General actions — Accidental actions; 2006.

[8] ASCE-7 - American Society of Civil Engineers. ASCE-7: Minimum design loads and associated criteria for buildings and other structures; 2022.

[9] Department of Defense USA. Unified Facilities Criteria (UFC): Design of Buildings To Resist Progressive Collapse, 2016.

[10] Mpidi Bita H, Huber JAJ, Voulpiotis K, Tannert T. Survey of contemporary practices for disproportionate collapse prevention. Eng Struct 2019;199:109578. https://doi.org/10.1016/j.engstruct.2019.109578.

[11] Russell JM, Sagaseta J, Cormie D, Jones AEK. Historical review of prescriptive design rules for robustness after the collapse of Ronan Point. Structures 2019;20: 365–73. https://doi.org/10.1016/j.istruc.2019.04.011.

[12] Svatoš-Ražnjević H, Orozco L, Menges A. Advanced Timber Construction Industry: A Review of 350 Multi-Storey Timber Projects from 2000–2021. Buildings 2022; 12:404. https://doi.org/10.3390/buildings12040404.

[13] Huber JAJ, Ekevad M, Girhammar UA, Berg S. Structural robustness and timber buildings – a review. Wood Mat Sci Eng 2019;14(2):107–28. https://doi.org/10.1080/17480272.2018.1446052.

[14] Arup. Review of international research on structural robustness and disproportionate collapse. London; 2011.

[15] Fast P, Gafner B, Jackson R, Li J. Case study: An 18 storey tall mass timber hybrid student residence at the University of British Columbia, Vancouver. World Conf. Timber Eng. 2016, Vienna; 2016.

[16] Wells M. Tall timber buildings: Applications of solid timber construction in multistory buildings. CTBUH J 2011:24–7.

[17] Milner MW, Edwards S, Turnbull DB, Enjily V. Verification of the robustness of a six-storey timber-frame building. Struct Eng 1998;76:307–12.

[18] Malo KA, Abrahamsen RB, Bjertnæs MA. Some structural design issues of the 14-storey timber framed building "Treet" in Norway. Eur J Wood Wood Prod 2016;74 (3):407–24. https://doi.org/10.1007/s00107-016-1022-5.

[19] Mpidi Bita H, Huber J, Palma P, Tannert T. Prevention of Disproportionate Collapse for Multistory Mass Timber Buildings: Review of Current Practices and Recent Research. J Struct Eng 2022:148. https://doi.org/10.1061/(ASCE)ST.1943-541X.0003377.

[20] Mpidi Bita H, Tannert T. Disproportionate collapse prevention analysis for a mid-rise flat-plate cross-laminated timber building. Eng Struct 2019;178:460–71. https://doi.org/10.1016/j.engstruct.2018.10.048.

[21] Mpidi Bita H, Currie N, Tannert T. Disproportionate collapse analysis of mid-rise cross-laminated timber buildings. Struct Infrastruct Eng 2018;14(11):1547–60. https://doi.org/10.1080/15732479.2018.1456553.

[22] Mpidi Bita H, Tannert T. Tie-force procedure for disproportionate collapse prevention of CLT platform-type construction. Eng Struct 2019;189:195–205. https://doi.org/10.1016/j.engstruct.2019.03.074.

[23] Mpidi Bita H, Tannert T. Numerical Optimisation of Novel Connection for Cross-laminated Timber buildings. Eng Struct 2018;175:273–83. https://doi.org/10.1016/j.engstruct.2018.08.020.

[24] Mpidi Bita H, Tannert T. Experimental Study of Disproportionate Collapse Prevention Mechanisms for Mass-Timber Floor Systems. J Struct Eng 2020;146(2): 04019199. https://doi.org/10.1061/(ASCE)ST.1943-541X.0002485.

[25] Huber JAJ, Mpidi Bita H, Tannert T, Berg S. Finite element analysis of alternative load paths to prevent disproportionate collapse in platform-type CLT floor systems. Eng Struct 2021;240:112362. https://doi.org/10.1016/j.engstruct.2021.112362.

[26] Huber JAJ, Ekevad M, Girhammar UA, Berg S. Finite element analysis of alternative load paths in a platform-framed CLT building. Proc Inst Civ Eng - Struct Build 2020;173(5):379–90. https://doi.org/10.1680/jstbu.19.00136.

[27] Mpidi Bita H, Malczyk R, Tannert T. Alternative Load Path Analyses for Mid-Rise Post and Beam Mass Timber Building. Struct Congr 2020;2020:72–80. https://doi.org/10.1061/9780784482896.008.

[28] GSA. General services administration alternate path analysis & design guidelines for progressive collapse resistance; 2013.

[29] Cao AS, Palma P, Frangi A. Column removal analyses of timber structures – Framework to assess dynamic amplification factors for simplified design methods. In: World conf timber eng; 2021, Online: 2021.

[30] Abrahamsen R, Bjertnæs MA, Bouillot J, Brank B, Cabaton L, Crocetti R, et al. Dynamic response of tall timber buildings under service load – The dynattb research program. In: Proc XI int conf struct dyn. (EURODYN 2020); 2020. https://doi.org/10.47964/1120.9397.18405.

[31] Schmid J, Voulpiotis K, Klippel M. Robustness in fire – possibilities for tall timber buildings. World Conf Timber Eng 2021;2021.

[32] Przystup AC, Lu Y, Reynolds T. Are current robustness design strategies appropriate for large timber structures? World Conf Timber Eng 2021;202:1.

[33] Zhang B, Zhao X, Kilpatrick T, Sandersaon I. Numerical simulations of disproportionate collapses of tall timber buildings under fire conditions using FEM. World Conf Timber Eng 2021;2021.

[34] Lyu CH, Gilbert BP, Guan H, Underhill ID, Gunalan S, Karampour H, et al. Experimental collapse response of post-and-beam mass timber frames under a quasi-static column removal scenario. Eng Struct 2020;213:110562. https://doi.org/10.1016/j.engstruct.2020.110562.

[35] Lyu CH, Gilbert BP, Guan H, Underhill ID, Gunalan S, Karampour H. Experimental study on the quasi-static progressive collapse response of post-and-beam mass timber buildings under an edge column removal scenario. Eng Struct 2021;228: 111425. https://doi.org/10.1016/j.engstruct.2020.111425.

[36] Lyu CH, Gilbert BP, Guan H, Underhill ID, Gunalan S, Karampour H. Experimental study on the quasi-static progressive collapse response of post-and-beam mass timber buildings under corner column removal scenarios. Eng Struct 2021;242: 112497. https://doi.org/10.1016/j.engstruct.2021.112497.

[37] Cheng X, Gilbert BP, Guan H, Underhill ID, Karampour H. Experimental dynamic collapse response of post-and-beam mass timber frames under a sudden column removal scenario. Eng Struct 2021;233. https://doi.org/10.1016/j.engstruct.2020.111425.

[38] Dietsch P. Robustness of large-span timber roof structures — Structural aspects. Eng Struct 2011;33(11):3106–12. https://doi.org/10.1016/j.engstruct.2011.01.020.

[39] Leijten AJM. Requirements for moment connections in statically indeterminate timber structures. Eng Struct 2011;33(11):3027–32. https://doi.org/10.1016/j.engstruct.2011.03.014.

[40] Buchanan A, Moss P, Wong N. Ductile moment-resisting connections in glulam beams. In: "Future Dir. a Vis. Earthq. Eng. New Zealand" 2001 annu conf proc NZ soc earthq eng, Wairakei, New Zealand; 2001. p. 9.

[41] Jorissen A, Fragiacomo M. General notes on ductility in timber structures. Eng Struct 2011;33(11):2987–97. https://doi.org/10.1016/j.engstruct.2011.07.024.

[42] Malo KA, Siem J, Ellingsbø P. Quantifying ductility in timber structures. Eng Struct 2011;33(11):2998–3006. https://doi.org/10.1016/j.engstruct.2011.03.002.

[43] Ottenhaus L-M, Jockwer R, van Drimmelen D, Crews K. Designing timber connections for ductility – A review and discussion. Constr Build Mater 2021;304: 124621. https://doi.org/10.1016/j.conbuildmat.2021.124621.

[44] Frangopol DM, Curley JP. Effects of damage and redundancy on structural reliability. J Struct Eng 1987;113(7):1533–49. https://doi.org/10.1061/(ASCE)0733-9445(1987)113:7(1533).

[45] Fu G, Frangopol DM. Balancing weight, system reliability and redundancy in a multiobjective optimization framework. Struct Saf 1990;7(2-4):165–75. https://doi.org/10.1016/0167-4730(90)90066-X.

[46] Baker JW, Schubert M, Faber MH. On the assessment of robustness. Struct Saf 2008;30(3):253–67. https://doi.org/10.1016/j.strusafe.2006.11.004.

[47] Pereira Cabanas Gonçalves André J, Havbro Faber M. Proposal of guidelines for the evolution of robustness framework in the future generation of Eurocodes. Struct Eng Int 2019;29(3):433–42. https://doi.org/10.1080/10168664.2019.1599706.

[48] Starossek U, Haberland M. Disproportionate Collapse: Terminology and Procedures. J Perform Constr Facil 2010;24(6):519–28. https://doi.org/10.1061/(ASCE)CF.1943-5509.0000138.

[49] SIA 261: Swiss Society of Engineers and Architects (SIA). SIA 261: Einwirkungen auf Tragwerke. Zürich; 2014.

[50] SIA 265: Swiss Society of Engineers and Architects (SIA). SIA 265: Holzbau. Zürich; 2012.

[51] Müller K, Frangi A. Micro-notches as a novel connection system for timber-concrete composite slabs. Eng Struct 2021;245:112688. https://doi.org/10.1016/j.engstruct.2021.112688.

[52] Kreis B. Two-Way Spanning Timber-Concrete Composite Slabs made of Beech Laminated Veneer Lumber with Steel Tube Connection. ETH Zürich 2021. https://doi.org/10.3929/ethz-b-000475052.

[53] KBOB. Ökobilanzdaten im Baubereich; 2016.

[54] JCSS. Joint Committee on Structural Safety Probabilistic Model Code; 2002.

[55] Deutsches Institut für Bautechnik. European Technical Assessment ETA-12/0063 of 17 July 2018; 2018.

[56] Johansen KW. Theory of timber connections. Int Assoc Bridg Struct Eng 1949;9: 249–62.

[57] CEN. TC 250 (N2579) bonded-in-rods; 2020.

[58] ETA-Danmark A/S. European technical assessment ETA-11/0496 of 2018/11/06. 2018.

[59] Rothoblaas. Rothoblaas TITAN V angle bracket technical sheet; 2018.

[60] fib Model Code 2010 - The International Federation for Structural Concrete (fib). fib Model Code 2010. Lausanne; 2010.

[61] Dassault Systemes Simulia Corporation. Abaqus 2021 documentation; 2021.

[62] Dassault Systemes Simulia Corporation. Abaqus 2021 documentation: types of problems suited for Abaqus/Explicit; 2021.

[63] Cobb F. Structural engineer's pocket book. 3rd ed. CRC Press; 2017.

[64] Domaneschi M, Pellecchia C, De Iuliis E, Cimellaro GP, Morgese M, Khalil AA, et al. Collapse analysis of the Polcevera viaduct by the applied element method. Eng Struct 2020;214:110659. https://doi.org/10.1016/j.engstruct.2020.110659.

[65] Schilling S, Palma P, Steiger R, Frangi A, Zürich E. Probabilistic description of the mechanical properties of glued laminated timber made from softwood. In: Int netw timber eng res - meet fifty-four, online; 2021.

[66] Fahrni R. Reliability-based code calibration for timber in fire. ETH Zürich 2021. https://doi.org/10.3929/ethz-b-000475057.

[67] Breiman. Random Forests. Mach Learn 2001;45:5–32.

[68] Chawla NV, Bowyer KW, Hall LO, Kegelmeyer WP. SMOTE: Synthetic Minority Over-sampling Technique. J Artif Intell Res 2002;16:321–57. https://doi.org/10.1613/jair.953.

[69] Lemaître G, Nogueira F, Aridas C. Imbalanced-learn: A Python Toolbox to Tackle the Curse of Imbalanced Datasets in Machine Learning. J Mach Learn Res 2017;18: 1–5.

[70] Kohavi R. A study of cross-validation and bootstrap for accuracy estimation and model selection. In: Proc 14th int jt conf artif intell - vol. 2, Montreal, Quebec, Canada: Morgan Kaufmann Publishers Inc.; 1995, p. 1137–43.

[71] Pedregosa F, Varoquaux G, Gramfort A, Michel V, Thirion B, Grisel O, et al. Scikit-learn: Machine Learning in Python. J Mach Learn Res 2011;12:2825–30. https://doi.org/10.1289/EHP4713.

[72] Scornet E. Trees, forests, and impurity-based variable importance; 2020.

[73] ID SIS HPC. Euler Cluster; 2021. https://scicomp.ethz.ch/wiki/Euler [accessed August 30, 2021].
[74] Kiakojouri F, Biagi V De, Chiaia B, Reza M. Progressive collapse of framed building structures: Current knowledge and future prospects, vol. 206; 2020. https://doi.org/10.1016/j.engstruct.2019.110061.
[75] Moustapha M, Marelli S, Sudret B. Active learning for structural reliability: Survey, general framework and benchmark. Struct Saf 2022;96:102174. https://doi.org/10.1016/j.strusafe.2021.102174.
[76] Benner P, Gugercin S, Willcox K. A survey of projection-based model reduction methods for parametric dynamical systems. SIAM Rev 2015;57(4):483–531. https://doi.org/10.1137/130932715.
[77] Kapteyn MG, Knezevic DJ, Willcox KE. Toward predictive digital twins via component-based reduced-order models and interpretable machine learning. AIAA Scitech 2020 Forum, Orlando: American Institute of Aeronautics and Astronautics; 2020. https://doi.org/10.2514/6.2020-0418.